THE FLORIDA STATE UNIVERSITY

COLLEGE OF ARTS AND SCIENCES

A SIMULATION OF THE BIOLOGICAL RESPONSE TO LOW-FREQUENCY PHYSICAL FORCING IN THE TROPICAL PACIFIC OCEAN

By

ANNETTE SAMUELSEN

A Thesis submitted to the
Department of Oceanography
in partial fulfillment of the
requirements for the degree of
Masters of Science

Degree Awarded:

Spring Semester 2000

The members of the Committee approve the thesis of Annette Samuelsen defended on 12/1/2000

Dr. James J. O Brien
Professor Directing Thesis

Dr. George Weatherly
Committee Member

Dr. Richard Iverson
Committee Member

Approved:

Dr. David Thistle, Chair, Department of Oceanography

Dr. Donald J. Foss, Dean, College of Arts and Sciences

Dr. Donald J. Foss, Dean, College of Arts and Sciences

ACKNOWLEDGEMENTS

I would like to thank my advisor Dr. O'Brien for his help, encouragement, and last but not least, enthusiasm during the course of doing the research for and writing this thesis. Dr. Michael Toner developed of the model that was used and he also introduced me to the model. I also acknowledge my committee members, especially Dr. Iverson for answering my questions about the biological system and marine biology in general. Steve Morey proofread my manuscript and gave many useful suggestions. Finally, I'm gratefull to my roommate Petya, who was very patient with me in periods my thesis was taking up all my energy.

Parts of this work were done while on a fellowship from the School of Computational Science and Information Technology, Florida State University.

TABLE OF CONTENTS

LIST OF TABLES

LIST OF FIGURES

The annual cycle in the central Pacific of (a) each biological component, (b) each biological component scaled by its own mean value, and (c) the primary and secondary productivity and vertical velocity.

1981 through 1985 at 110° W in the eastern Pacific on the equator of (a) ammonium, (b) detritus, (c) nitrate, (d) phytoplankton, and (e) zooplankton. Note the difference in the solutions of ammonium and zooplankton after 1983.

130 degrees West in the period from 1982 through 1985. A large-amplitude upwelling Kelvin wave is arriving at the coast of South America the end of 1983 and Rossby waves

ABSTRACT

A biological model is coupled to a 1 1/2 layer reduced gravity physical ocean-model. The model is calculated for 35 years in the tropical Pacific Ocean in the domain encompassing 20° S to 25° N and 124° E to 74° W. The physical model is forced by the FSU monthly winds and has realistic coastlines on the eastern and western side of the domain. The biological model has five components: phytoplankton, zooplankton, nitrate, ammonium, and detritus and uses realistic parameters. Some of the processes included in the model are bacterial action, iron-limitation, and nutrient regeneration. The aim of the study is to investigate the biological response to physical forcing on the time scales of annual to inter-annual time scales. While phytoplankton seem to immediately respond to the forcing from physical model, zooplankton is the component that shows the most variability on longer time scales.

The annual cycle is derived from the first 16 years of model-data. Three regions show persistent high productivity: the Equatorial Cold Tongue, a region in the central Pacific around 9° N and a region close to the western boundary at approximately 6° N. The north-south movement of the ITCZ influences the annual cycle in the eastern and central Pacific, both in terms of local forcing and in terms of remote forcing through equatorial waves. The high production in the western Pacific is connected to a series of eddies generated by the shear between the North Equatorial Current and the North

Equatorial Counter Current. The mean state in the model shows a marked asymmetry across the equator. The region North of the equator is much more productive than the region south of the equator except in the equatorial Cold Tongue. The reason is that the ITCZ stays north of the equator and causes the upper-layer depth to be shallower north of the equator.

The period during and after the 1982-83 El Ni o in the eastern pacific shows anomalously low stocks of zooplankton and productivity in the eastern Pacific. In the period after 1983 there is anomalously high production that persists almost two years. A strong upwelling Kelvin wave is responsible for adding an excess of nitrate which contributes to increasingly large production late in 1983. In a period of over a year after that a series of inter-seasonal Kelvin waves keep the production high in the eastern Pacific. At the same time a series of Rossby-waves propagate westward across the Pacific. The Rossby waves enhance the biological production as they propagate across the basin, and their signal can be followed all the way to the western boundary. Thus the signal from the Rossby and Kelvin waves can be detected in all the biological components as well as in the thermocline.

1. INTRODUCTION

The interaction between the living organism and its physical environment is of interest in ecosystems both in the ocean and on land. It is becoming increasingly important to understand this interaction in view of the human environmental influence. One topic that requires the understanding of the interaction between physics and biology in the ocean is climate prediction, i.e. how global warming will affect biological production and how this change will give a feedback to the climate system. On a global scale the ocean is a large sink of atmospheric carbon [*Matear and Hirst,* 1999]. The amount absorbed is dependent on biological production as well as physical factors. The export of carbon dioxide to the deeper ocean happens through the sinking of fecal pellets, which contain organic carbon that has been sequestered from atmospheric carbon. Although carbon dioxide is lost from the ocean in equatorial upwelling regions, the production in the area contributes to export of carbon to the deep ocean on a global scale. Thus knowing the primary and secondary productivity in addition to physical ocean processes is important in climate modeling. Also the influence of natural interannual oscillations and their impact on biological production has a large impact on the economy in many countries, because their income depends on fisheries. Understanding the interaction between the physical ocean and its ecology is thus also of interest to the
in many countries, because their income depends on fisheries. Understanding the interaction between the physical ocean and its ecology is thus also of interest to the fishery industry [*Cushing*, 1995].

One approach to study the interaction between the ocean and its organisms is to use a marine ecosystem model coupled to a physical model. There are two main approaches to model ecosystems mathematically: one is based on the flow of energy through the ecosystem, the other is based on the concept of a limiting nutrient, e.g. phosphorus, iron or, as in this case, nitrogen. The earliest marine biological models were simple two or three component models that were developed from classical predator-prey equations. These were not coupled with an explicit physical model, but used an observed annual cycle of the mixed layer or nutrient concentration or a simple injection of nutrients due to of the change with season. *Fleming* [1939] and *Cushing* [1959] developed some of the first plankton models. Recently most of the coupled physical-biological models have detailed mixed layer structure, but little or no horizontal extent [e.g., *Fasham et al.*, 1990; *K hn and Radach,* 1997; *Loukos et al.1997*]. More complicated model were developed by *Leonard et al.* [1999] and *McClain, et al.*[1999] who coupled a 9-componet ecosystem model to a mixed layer model in the equatorial Pacific. *Sarmiento et al.,* [1993] coupled a biological model with a general circulation ocean model in the Atlantic Ocean. Other examples of three-dimensional models coupled with biological models are *Chai et. al.* [1996] and *Toggweiler and Carson* [1996]. Data assimilation has also been used to make the biological models more realistic [*Spitz*, 1996; *Friedrichs*, 1999]. *Koziana* [1999] used a model to investigate how phytoplankton influences heating of the surface mixed-layer. A review of a several coupled physical-biological models from the very simple ones to the more complicated is given by *Olson and Hood* [1994].

A concept that has been widely studied after it became clear that it is important is very simple ones to the more complicated is given by *Olson and Hood* [1994].

A concept that has been widely studied after it became clear that it is important is iron limitation. Iron limitation has the effect of inhibiting the uptake of nitrate, i.e. new

production, but not of ammonium or regenerated nutrients. Iron is usually considered to be transported to the ocean by atmospheric dust. However, the central tropical Pacific does not have a significant atmospheric source since the prevailing westward trades do not originate over much land. Iron can also be transported into the mixed layer from the deep ocean. In particular the Equatorial Cold Tongue gets its supply of iron from the Equatorial Under Current. Iron limitation has studied using shipboard bottle experiments [*Martin and Fitzwater,* 1988], mesoscale iron enrichment experiments [*Coale et al.* 1998] and through the use of marine ecosystem models [*Chai et al*, 1995]. As a result of iron limitation the tropical Pacific, unlike other ocean regions, usually has excess nitrate in the surface layer. *Landry et al.* [1997] concluded that iron-deficiency combined with grazing is responsible for high nutrients and low chlorophyll conditions in the tropical Pacific Ocean. In this model, the iron-limitation process is not explicitly modeled, but parameterized into the model by adjusting the parameters that determine uptake of nutrients.

Physical processes on all time scales influence life in the ocean. These processes have in common that they regulate the amount of nutrients or the availability of light in the euphotic zone. Turbulence is responsible for mixing of nutrients into the upper boundary layer. Coastal upwelling is responsible for some of the most productive areas along the coast, while equatorial upwelling is responsible for the productivity in the equatorial regions. Planetary waves alter the depth of the thermocline and thus increase and decrease the flux of nutrients into the mixed layer. The smaller animals and plants respond rapidly to the change in the physical environment. Larger organisms will have to

and decrease the flux of nutrients into the mixed layer. The smaller animals and plants respond rapidly to the change in the physical environment. Larger organisms will have to relocate or find other sources of food or better breeding ground. Larger organisms also

respond slower to environmental changes because they take more time to reproduce. The role of equatorial waves in connection with oceanic primary production became apparent during the 1982 El Niño. After the 1982/83 El Niño it was noted the reduced production in the eastern Pacific during this time was caused by a remotely forced downwelling Kelvin wave. If the thermocline is too deep, upwelling will not bring nutrient-rich water from below the thermocline into the euphotic layer [*Barber and Chavez*, 1983].

In this study a five component marine ecosystem model is coupled to a 1 1/2-layer reduced-gravity ocean-model. The model-domain spans the entire tropical Pacific Ocean and the model is run for 35 years in the period from 1961 to1996. The physical model is forced by the FSU monthly winds and the output from this model is used to force the ecological model. The ecosystem model has five components: zooplankton, phytoplankton, nitrate, ammonium, and detritus. The biological model equations are integrated over the mixed layer so the model only resolves horizontal structure. The model also uses a unique semi-Lagrangian advection scheme, which eliminates the requirement for horizontal boundary conditions at shores for the biological model. The object of this study is to investigate the biological response to physical forcing on long time scales. The main focus is on the annual cycle and the effect of ENSO. In order to keep the model as simple as possible, light is not used as a variable in the model. In most marine environments nitrate is the limiting nutrient, and is supplied from the deep ocean in this model.

The simulation is used to study the annual cycle and the impact of ENSO on the biological production, even though monthly forcing is used. The annual cycle is

The simulation is used to study the annual cycle and the impact of ENSO on the biological production, even though monthly forcing is used. The annual cycle is calculated to determine if the model exhibits an annual cycle and to determine what

drives the annual cycle. On ENSO time scales the strong 1982-84 ENSO event is investigated. This event was chosen because it has a strong ENSO signal and because the biological solutions show a dramatic change in character over this period. Another interesting aspect is the effect of equatorially trapped waves. These waves have a large impact on both primary and secondary productivity and can be detected across the entire ocean basin.

A detailed description of the model is given in section 2. The results are presented in section 3. The annual cycle of the biological components is calculated and explained in terms of the forcing and oceanic response. The impact of ENSO on the biological system is investigated by focusing on the 1982-83 El Niño and 1984 La Niña. The model shows a change of character during this period, which can be explained in terms of a combination of interannual, and interseasonal equatorial Kelvin waves. Discussion and conclusions are presented in section 4. A discussion of the parameterization of vertical nitrate-flux is given in appendix A and a description of the semi-Lagrangian advection-scheme is given in appendix B.

2. MODEL DESCRIPTION

The model consist of two parts, a nonlinear reduced gravity physical model that is forced by the monthly FSU winds and a marine ecosystem model that is forced by the velocity data from the physical model. The physical processes affect the biological system, but the biological variables do not give feedback to the physical model. Therefore the coupling is only one-way; A new semi-Lagrangian biological advection scheme is used in the biological model. The ecosystem has two nitrogen nutrients (nitrate and ammonium), phytoplankton, zooplankton, and detritus. Important biological processes such as iron-limitation, regeneration of nutrients by bacterial action, and sinking are parameterized in the model. Because the goal is to study variations on long time scales the daily light cycle is not included in this model. The seasonal light dependence is also neglected since the model is applied to the tropics, where the amount of light does not change much with season. Each biological equation is averaged over the surface mixed layer, so the model only captures the horizontal and temporal structure

2.1. Physical model

The physical model is a nonlinear, 1 1/2-layer, reduced gravity ocean-model and spans the entire tropical Pacific Ocean. The model is governed by the following equations:

$$\frac{\partial U}{\partial t} + \frac{1}{a\cos\theta}\frac{\partial}{\partial\phi}\left(\frac{U^2}{h}\right) + \frac{1}{a}\frac{\partial}{\partial\theta}\left(\frac{UV}{h}\right) - (2\Omega\sin\theta)V + \frac{g' h}{a\cos\theta}\frac{\partial h}{\partial\phi}$$

$$-\frac{\tau^{\phi}}{\rho} - \frac{A}{a^2\cos^2\theta}\left[\frac{\partial^2}{\partial\phi^2} + \cos\theta\frac{\partial}{\partial\theta}\left(\cos\theta\frac{\partial}{\partial\theta}\right)\right]U = 0 \qquad (1)$$

$$\frac{\partial V}{\partial t} + \frac{1}{a\cos\theta}\frac{\partial}{\partial\phi}\left(\frac{UV}{h}\right) + \frac{1}{a}\frac{\partial}{\partial\theta}\left(\frac{V^2}{h}\right) + (2\Omega\sin\theta)U + \frac{g' h}{a\cos\theta}\frac{\partial h}{\partial\theta}$$

$$-\frac{\tau^{\theta}}{\rho} - \frac{A}{a^2\cos^2\theta}\left[\frac{\partial^2}{\partial\phi^2} + \cos\theta\frac{\partial}{\partial\theta}\left(\cos\theta\frac{\partial}{\partial\theta}\right)\right]V = 0 \qquad (2)$$

$$\frac{dh}{dt} + \frac{1}{a\cos\theta}\left[\frac{\partial U}{\partial\phi} + \frac{\partial}{\partial\theta}(V\cos\theta)\right] \qquad (3)$$

In these equations U is the zonal upper layer transport, V is the meridional upper layer transport, and h is the upper-layer depth. The parameters in the model are g', the reduced gravity constant; A, the horizontal eddy viscosity; and ρ, the upper layer density. The parameter values are given in Table 1. Longitude and latitude are denoted by ϕ and θ, respectively, and τ^{ϕ} and τ^{θ} are the estimated zonal and meridional wind stresses. The parameter a represents the radius of the earth and Ω the angular speed of the earth. The model is integrated on a sphere from 20° S to 25° N and 124° E to 74° W (Figure 1) using an Arakawa C-grid. The time step in the model is 30 minutes and the spatial resolution is 0.125° [*Kamachi and O'Brien*, 1995]. The model has irregular but realistic eastern and western boundaries. Radiation open boundary conditions are applied to the north and the south boundary [*Camerlengo and O'Brien*, 1996]. The western boundary is closed, so there is no though-flow to the Indian ocean. Closing this boundary does not have a significant effect on the Pacific Ocean at low frequencies in this type of model [*Verschell et al.*, 1995]. The model provides fields of U, V, and h every 10 days from 1961 through 1996 on a 1/4° grid. These data are used to force the biological model.

Table 1. The parameters and parameter-values used in the physical model

Parameter description	Parameter symbol	Value
Reduced gravity constant	g'	0.02 m/s^2
Horizontal eddy viscosity	A	750 m^2/s
Upper layer density	ρ	1025 kg/m^3

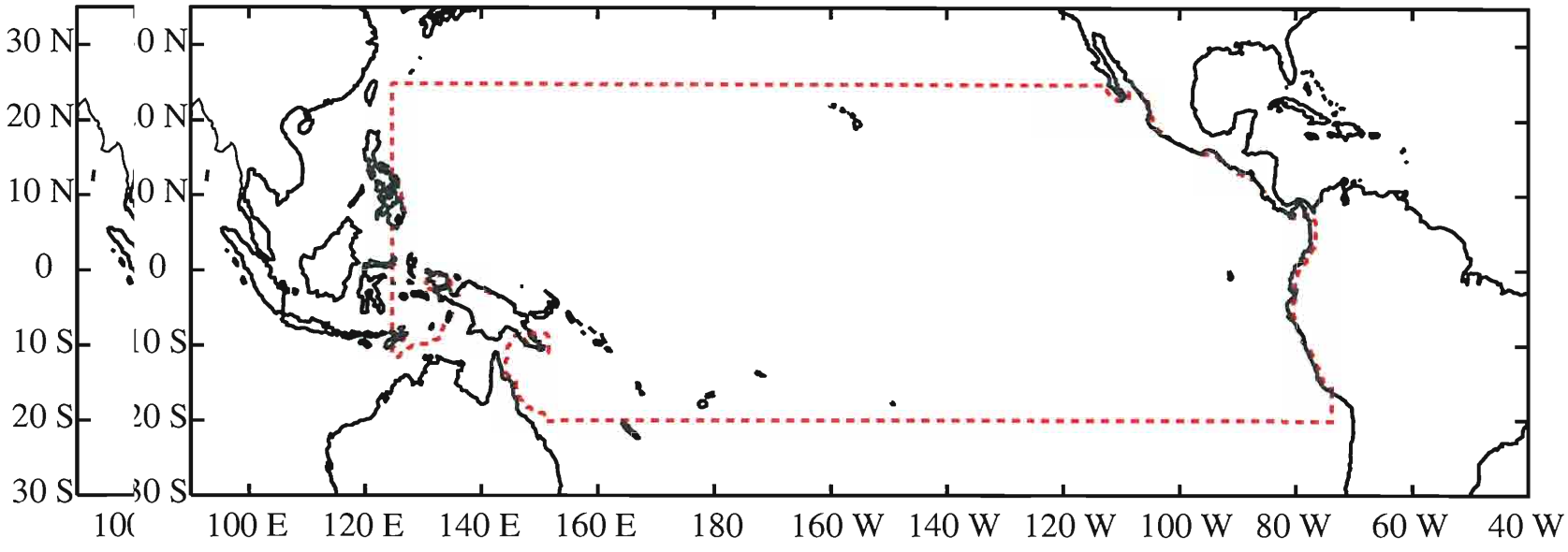

Figure 1.Figure 1. Map over the model domain. The area inside the dashed curve is the model domain, it extends from 124 degrees edegrees east to 74 degrees west and from 20 degrees south to 25 degrees north, and has realistic coastlines on the easterthe eastern and the western boundaries.

2.2. Biological model

The biological model has five components: zooplankton, phytoplankton, ammonium, nitrate, and detritus. In the model equations each component is non-dimensionalized with respect to deep-water nitrate concentration and integrated over the mixed layer. In other words the sum of the scaled concentration of deep-water nitrate is unity and the model-solutions have values given in fraction of deep-water nitrate concentration. The depth of the mixed layer is constant in the model. In this simulation it is 75 m. Data of upper-layer depth are used to determine the amount of nutrients entering the mixed layer. Horizontal advection is calculated using upper layer physical model transports. The time unit in the model is 1 day and the time-step is 1/10 day. This time step is computationally stable and yields good accuracy since the fastest time scale is about one day. Figure 2 gives an overview of the biological model.

2.2.1. Zooplankton

The zooplankton equation is:

$$\frac{DZ}{Dt} = (\Gamma(P) - m - T)Z \qquad (4)$$

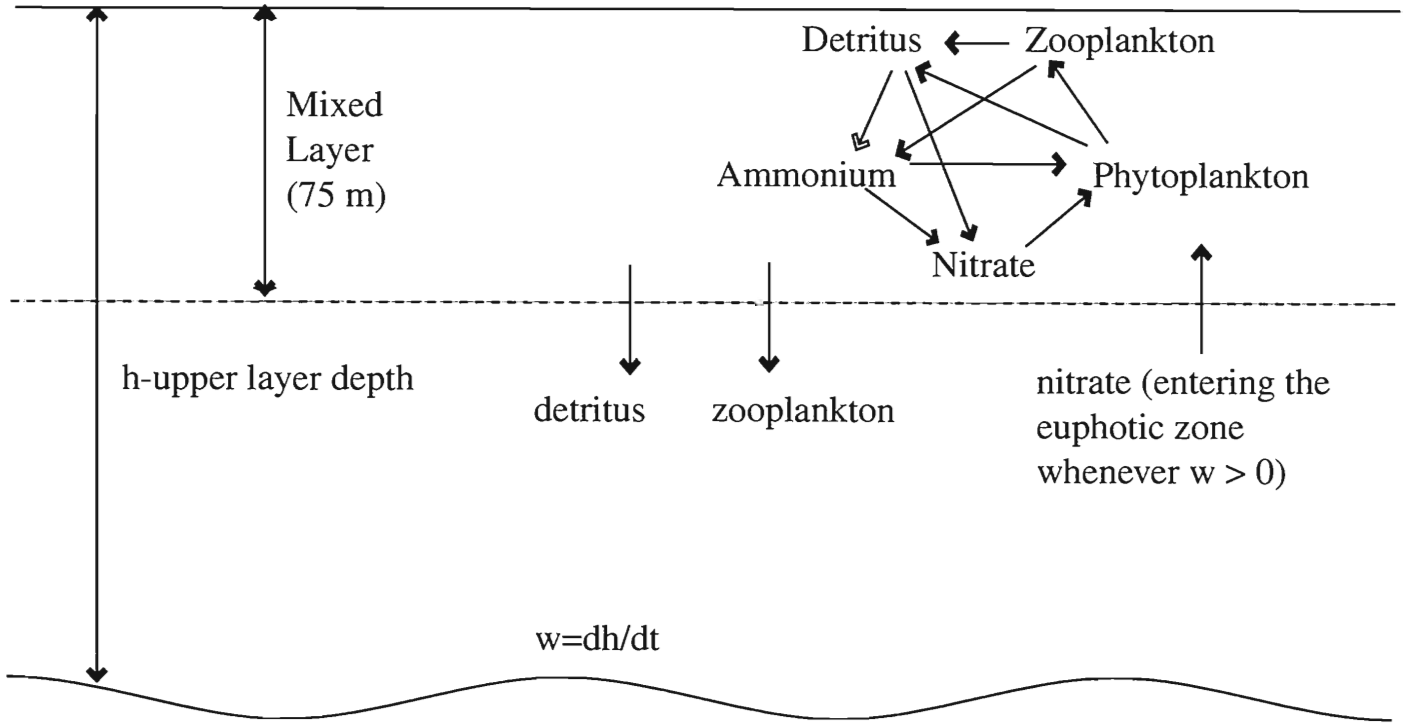

Figure 2. Overview over the dynamics of the biological model and how it interacts with the physical model.

In the zooplankton equation Z in the non-dimensional zooplankton concentration and m is the zooplankton sinking rate; mZ is the loss from the system. Values of the parameters in the biological model are given in Table 2. T is a function of biological processes and represents zooplankton mortality. A fraction of the dead zooplankton enters the detritus pool, which eventually sinks or is regenerated by bacteria to nutrients. The other fraction is directly regenerated into ammonium. The values of T and m, are 0.04 day^{-1} and 0.01 day^{-1} respectively, which means that zooplankton population decays on a e-folding time-scale of 20 days [1]. Grazing on phytoplankton is modeled by the Ivlev grazing function $\Gamma(P)$ [*Ivlev,* 1961].

$$\Gamma(P) = \Gamma_{max}(1 - \exp(\Lambda(P_0 - P))) \quad (5)$$

Γ_{max} is the maximum grazing rate, and Λ is the Ivlev grazing constant. P_0 is the minimum phytoplankton population needed for zooplankton-growth. P_0 is zero in this model. For Γ_{max}=1.0 day^{-1}, Λ=2.0 and for a nominal value of phytoplankton, P = 0.02, zooplankton will be growing exponentially on a time-scale of 25 days. For a phytoplankton population of ~0.025 the zooplankton population will be almost steady and for any larger phytoplankton stock the zooplankton population will increase.

2.2.2. Phytoplankton

The phytoplankton equation is:

The phytoplankton equation is:

[1] An e-folding scale means that for a scale, a in days, an initial concentration is reduced to e^{-1} or approximately 1/3 in a days.

$$\frac{DP}{Dt} = (\gamma(N) + \delta(A) - \alpha)P - \Gamma(P)Z \qquad (6)$$

The parameter α represents phytoplankton senescence; dead phytoplankton biomass is added to the detritus pool. Phytoplankton nutrient uptake is modeled by Michaelis-Menten kinetics [*Dugdale and Goering*, 1967], and $\gamma(N)$ and $\delta(A)$ are the functions governing uptake of nitrogen and ammonium by phytoplankton. The term $\gamma(N)$ represents new production and the term $\delta(A)$ represents regenerated production. The equations for $\gamma(N)$ and $\delta(A)$ are given by:

$$\gamma(N) = \gamma_{max} \frac{N}{\kappa + N} \qquad (7)$$

$$\delta(A) = \delta_{max} \frac{A}{\lambda + A} \qquad (8)$$

Ammonium will be preferentially used by phytoplankton because the half-saturation constant, λ is lower than the half-saturation constant for nitrate, κ. Iron limitation is parameterized by increasing the value of the half-saturation constant for nitrate, κ, and keeping the of the half-saturation constant for ammonium. Iron is mostly supplied to the oceanic mixed layer by atmospheric dust, however the tropical Pacific has no significant atmospheric source of iron from the westward trade winds. Iron is also supplied from the deep ocean. This process is modeled by lowering the value of half-saturation constant for nitrate every time new nutrients are supplied to the system. The maximum uptake-rate of ammonium, δ_{max}, is higher than the maximum uptake rate of nitrate γ_{max}. Under optimal conditions phytoplankton can grow on a time-scale of 1 day using ammonium and on 1.2 days using nitrate. In absence of zooplankton, phytoplankton decays on a time-scale of ten days.

2.2.3. Detritus

The detritus equation is:

$$\frac{DD}{Dt} = \nu TZ + \alpha P - (\eta + s)D \qquad (9)$$

Dead phytoplankton and a fraction, ν, of dead zooplankton become detritus. In the detritus equation s is the sinking rate of detritus; sD is lost from the system. The fraction

Dead phytoplankton and a fraction, ν, of dead zooplankton become detritus. In the detritus equation s is the sinking rate of detritus; sD is lost from the system. The fraction η is recycled to nutrients. The values of s and η are both 0.1 day^{-1}, therefore the detritus

has a residence time of 5 days in the mixed-layer. When detritus is regenerated to nutrients, 50% is recycled to ammonium and 50% to nitrate

2.2.4. Ammonium

The ammonium equation is:

$$\frac{DA}{Dt} = (1 - \nu)TZ + \chi\eta D - \delta(A)P - \beta A \qquad (10)$$

A fraction of the dead zooplankton is directly regenerated to ammonium, another part becomes detritus before it is regenerated. Bacterial action transforms the fraction β of ammonium to nitrate. Because phytoplankton prefer ammonium over nitrate, ammonium tends to be cycled very fast. Under normal conditions the concentration of ammonium is always very low, while there is almost always leftover nitrate in the mixed layer.

2.2.5. Nitrate

The nitrate equation is:

$$\frac{DN}{Dt} = V(N,t) + (1 - \chi)\eta D - \gamma(N)P + \beta A \qquad (11)$$

Nitrate is recycled from detritus and ammonium, and used by phytoplankton. V(N,t) is the source term in the biological model, it represents the amount of new nutrients entering the mixed layer. A more detailed discussion of the expression for nitrate-flux is given in Appendix A. The expression for V(N,t) is:
entering the mixed layer. A more detailed discussion of the expression for nitrate-flux is given in Appendix A. The expression for V(N,t) is:

$$V(N,t) = \frac{1 - N(t)}{h(t) - d}\left(\frac{dh}{dt}\right)' \tag{12}$$

$$\left(\frac{dh}{dt}\right)' = \begin{cases} 0, & \frac{dh}{dt} \le 0 \\ \frac{dh}{dt}, & \frac{dh}{dt} \ge 0 \end{cases} \tag{14}$$

The biological model conserves mass exactly if sinking and V(N,t) are zero. This is expressed

$$\frac{d}{dt}(P + N + Z + A + D) = -\text{sinking} + V(N,t) \tag{15}$$

The operator $\frac{d}{dt}()$ is the substantial derivative in the horizontal.

$$\frac{d}{dt}() = \frac{\partial}{\partial t}() + u\frac{\partial}{\partial x}() + v\frac{\partial}{\partial y}() \tag{16}$$

Table 2. The parameters and parameter-values used in the biological model (M. Toner personal communication).

Parameter description	Parameter symbol	Value
Ivlev grazing constant	Λ	2.0
Zooplankton mortality	T	0.04 day^{-1}
Zooplankton sinking rate	m	0.01 day^{-1}
Maximum zooplankton grazing-rate	Γ_{max}	1.0 day^{-1}
Maximum nitrate uptake	γ_{max}	0.8 day^{-1}
Nitrate half-saturation constant (normal)	κ	0.1
Nitrate half-saturation constant (upwelling)	κ	0.07
Maximum ammonium uptake	δ_{max}	1 day^{-1}
Ammonium half-saturation constant	λ	0.02
Phytoplankton death rate	α	0.1 day^{-1}
Fraction of zooplankton $\rightarrow$ detritus	υ	0.1
Fraction of detritus $\rightarrow$ nutrients	η	0.1 day^{-1}
Detritus sinking rate	s	0.1 day^{-1}
Fraction of regenerated detritus $\rightarrow$ ammonium	χ	0.5
Bacterial action on ammonium	β	0.1

3. RESULTS

3.1. The mean state and the annual cycle

In mid-latitude marine ecosystems the annual cycle of plankton is to a large degree controlled by the availability of light. In the tropics, however, light and weather conditions are fairly steady over the year, so the other physical processes become more important.

We propose to answer the following questions about the annual cycle.

- Do the biological components exhibit an annual cycle?
- Which physical processes cause the annual cycle?

The annual cycle and the mean was calculated using model data from period 1964 through 1979 because the period after 1980 is dominated by strong ENSO-events. In the mean state three regions show persistent high zooplankton stocks (Figure 3a): the Equatorial Cold Tongue, the Central Pacific around 10 degrees north of the equator, and close to the western boundary around 6° N. The mean state of phytoplankton (Figure 3b) has a very different pattern from the zooplankton. It is almost symmetric around the equator, while the zooplankton pattern show higher concentration north of the equator.

The equatorial Cold Tongue is a region that is known to be very productive. Two large-scale processes can influence upwelling in this region: local wind forcing that

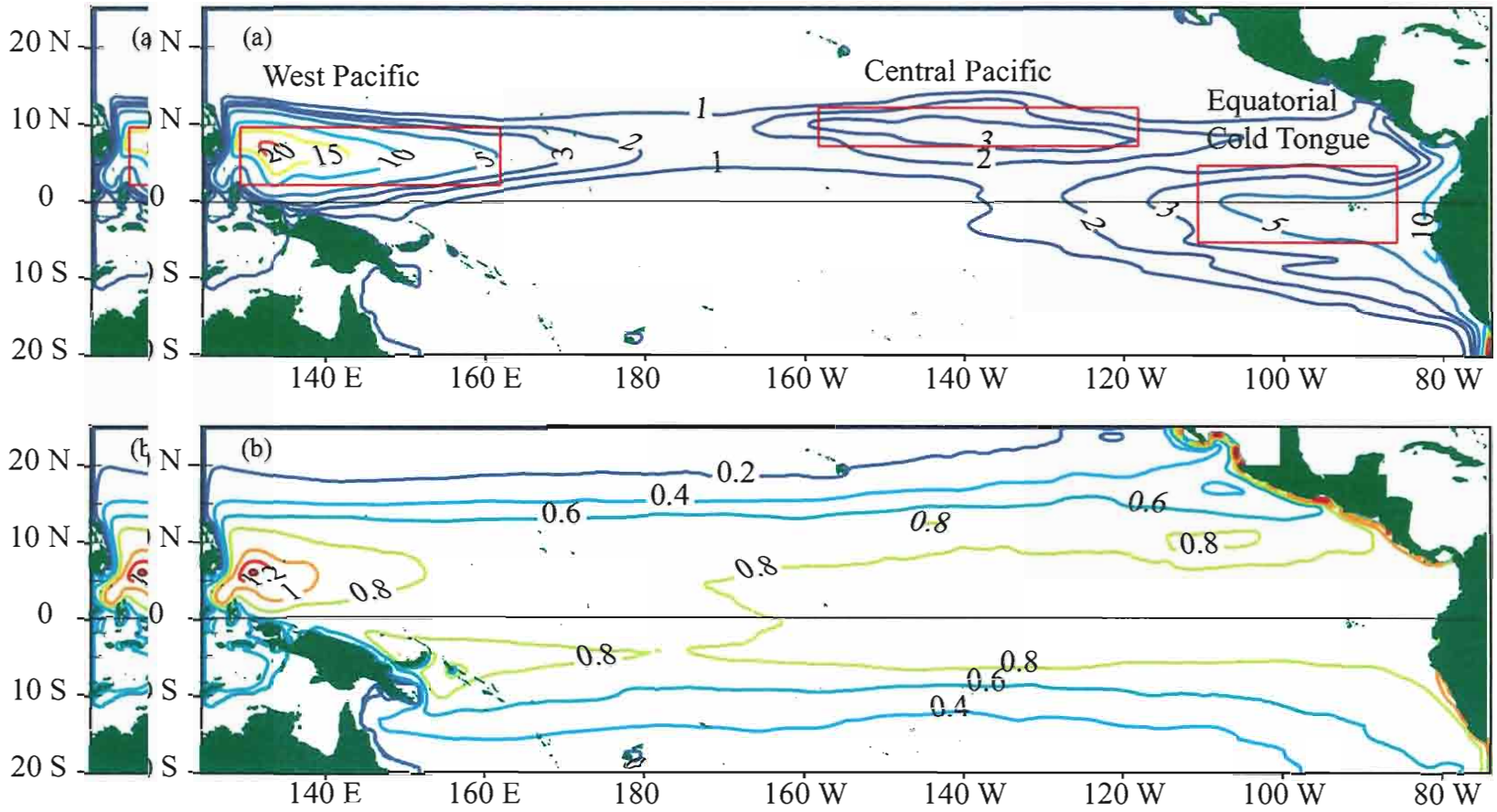

Figure 3. Figure 3. (a) The mean concentration of zooplankton (% of deep-water nitrogen-concentration) in the period from 1964 through 1979. Th 1979. The red boxes mark the regions we chose to study the annual cycle. (b) The mean concentration of phytoplankton (mg chla/l (mg chla/L) in the same period. Phytoplankton values were calculated using deep-water nitrate concentration of 25 mg/L, 5.6 mg C/ 5.6 mg C/ mg N, and 58 mg C/mg chla [Eppley, 1992].

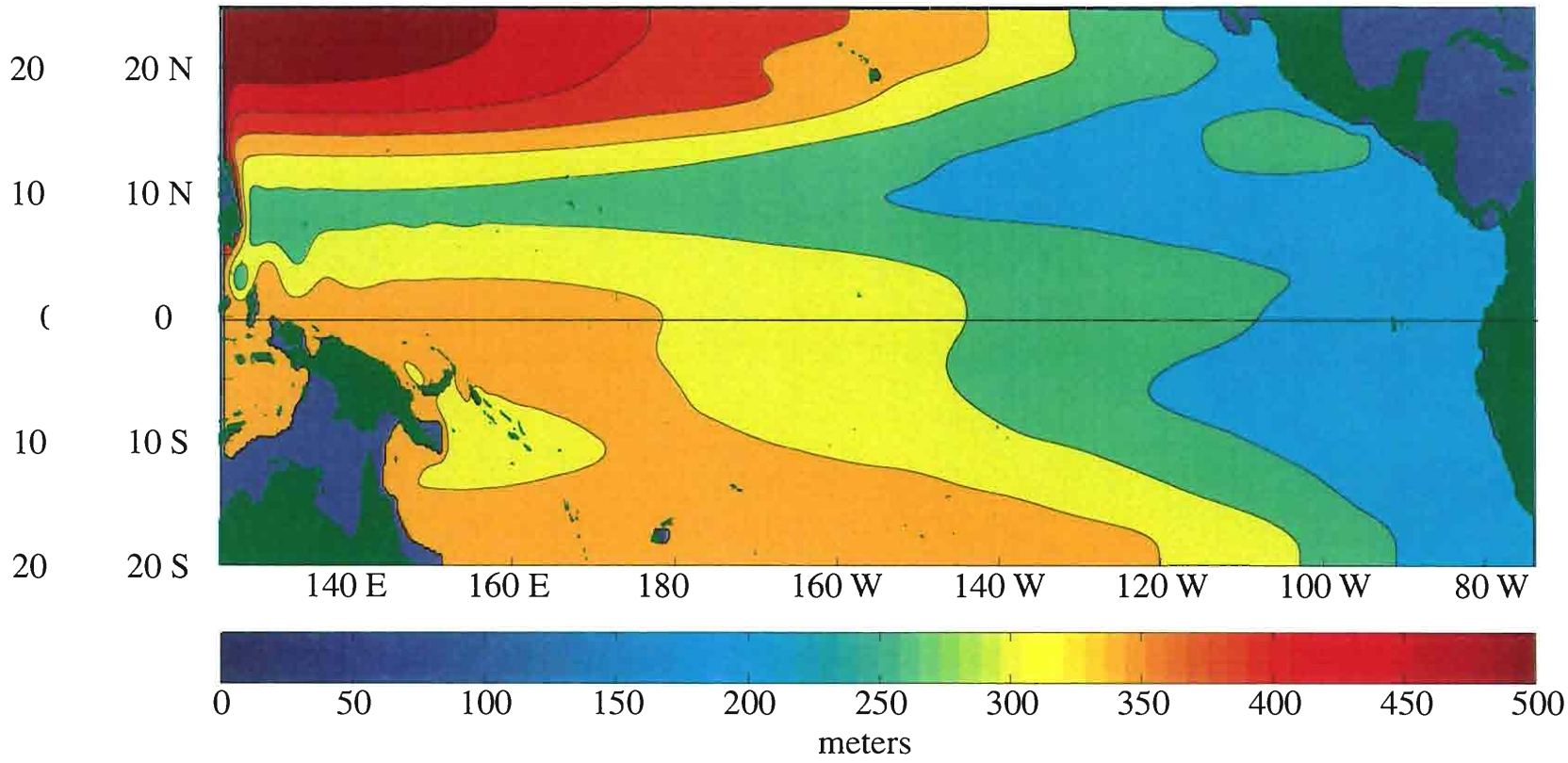

Fig **Figure 4.** The mean thermocline-depth in the model domain over the 16-year period. Note that the thermocline is
mu much shallower to the north of the equator than to the south.

generates equatorial and coastal upwelling and remotely generated equatorial Kelvin waves [*Barber,* 1988]. The region in the central Pacific around 9¡ N. has a shallow thermocline caused by divergence in the water masses just north of the ITCZ. Since the ITCZ resides north of the equator most of the time in the tropical Pacific, the upper layer is thinner north of the equator than south of the equator (Figure 4). Slow moving Rossby waves reflected from the eastern boundary also affect this region. The region in the western Pacific, around 6 degrees north was not expected to have large production. The highest productivity occur in the region between the North Equatorial Counter Current and the North Equatorial Current and the productivity in the region seems to be connected with eddies.

Since the high concentrations of zooplankton reflect high productivity, the annual cycle in each of these regions was analyzed. A box within each region was chosen to represent the region. The areas are marked with rectangles in Figure 3a.

3.1.1. Equatorial cold tongue

The equatorial cold tongue is a very productive region and is important to commercial fishing. The thermocline in the region is kept shallow by equatorial upwelling generated by the local westward winds. This process, which brings nutrient-rich water into the mixed-layer, also causes the region to be very productive. Kelvin waves also impact the region, they enhance or reduce the amount of nutrient-flux by raising or lowering the thermocline. The productivity should therefore be controlled by the magnitude of the westward wind-stress in the region, but also by remote wind forcing.

As seen in Figure 5c, the annual cycle has two peaks in productivity, one large in the magnitude of the westward wind-stress in the region, but also by remote wind forcing.

As seen in Figure 5c, the annual cycle has two peaks in productivity, one large in March and a smaller one around July. The productivity is least around December. The

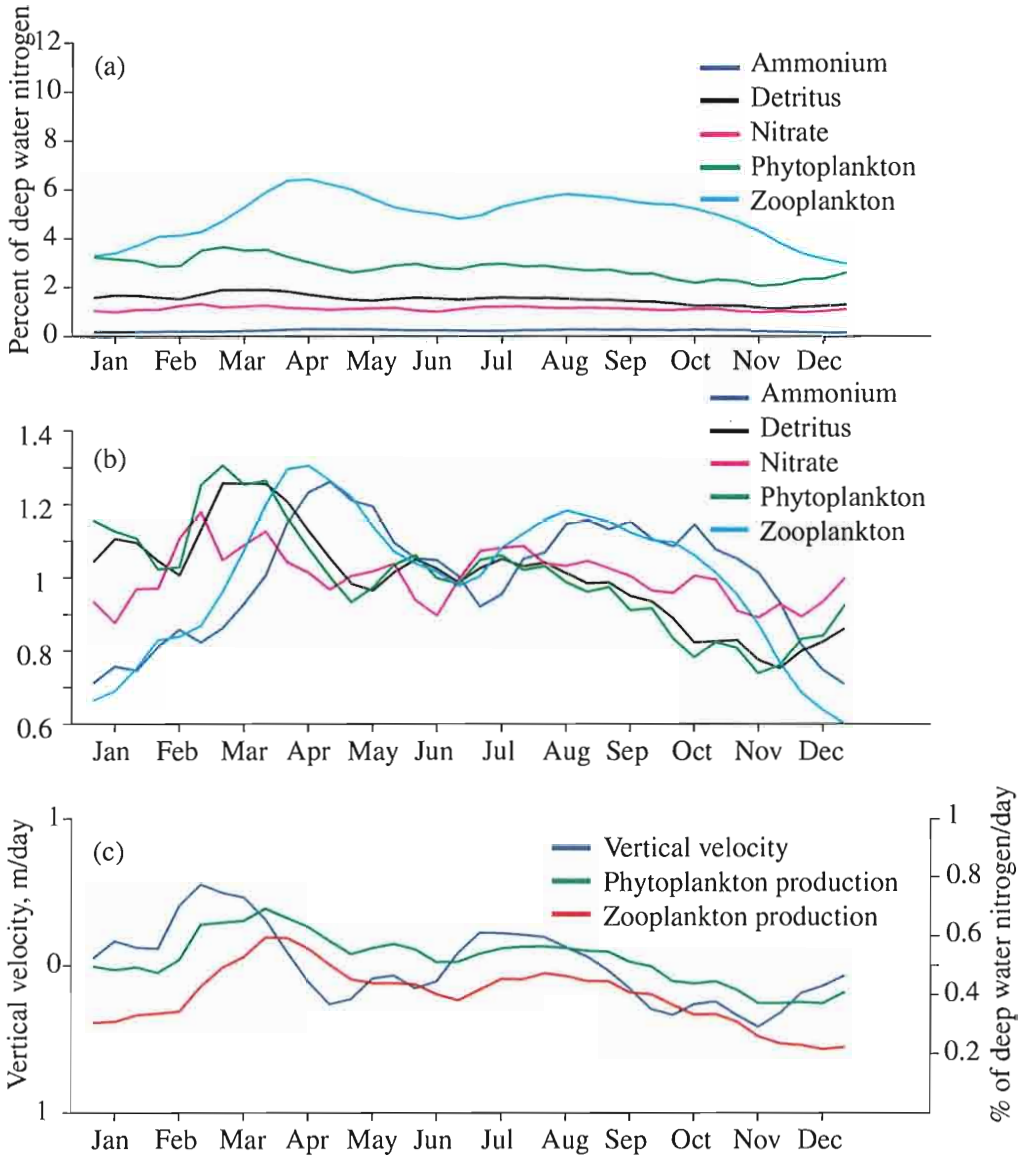

Figure 5. The annual cycle in the eastern Pacific of (a) each biological component, (b) each biological component scaled by its own mean value and, (c) the primary and secondary productivity and vertical velocity.

variation in production is mostly reflected in the zooplankton stock (Figure 5a). Phytoplankton shows a slight variation throughout the year, while the other components appear to stay on a very constant level. However, if each component is scaled by its mean value (Figure 5b) it becomes clear that both ammonium and detritus have distinct annual cycles. The phytoplankton stock increases almost simultaneously with the input of nutrients. The annual cycle of ammonium closely follows that of zooplankton. The annual cycle of phytoplankton and detritus are also very similar. The relatively large increase in phytoplankton stock in early spring after the winter is only possible because the zooplankton stock is too low to control the phytoplankton stock at this time of the year. The zooplankton stock grows quickly and reaches its maximum a little more than a month after the peak in phytoplankton. Throughout the rest of the year the zooplankton stock is large enough to keep the phytoplankton stock low. The very low concentration of ammonium reflects that ammonium is cycled very fast in the system while the leftover nitrate reflects the property of the model that nitrate uptake is inhibited. During most of the year primary production using ammonium is larger than production using nitrate, reflecting that regeneration of nutrients is an important factor in the productivity.

The production is largest in March, and the maximum upwelling occurs in February. In the western Pacific the ITCZ moves across the equator twice during the year [*Waliser and Gautier*, 1993], once in March and once in December. This gives rise to semiannual Kelvin waves. *Meyers* [1979] first brought up the idea that the seasonal cycle of the thermocline in the eastern Pacific was remotely forced. It was later discussed by *Busalacchi and O'Brien* [1980] and *Kindle* [1979]. During the year two upwelling cycle of the thermocline in the eastern Pacific was remotely forced. It was later discussed by *Busalacchi and O'Brien* [1980] and *Kindle* [1979]. During the year two upwelling Kelvin waves are generated west of the dateline, one in December and on in April (Figure

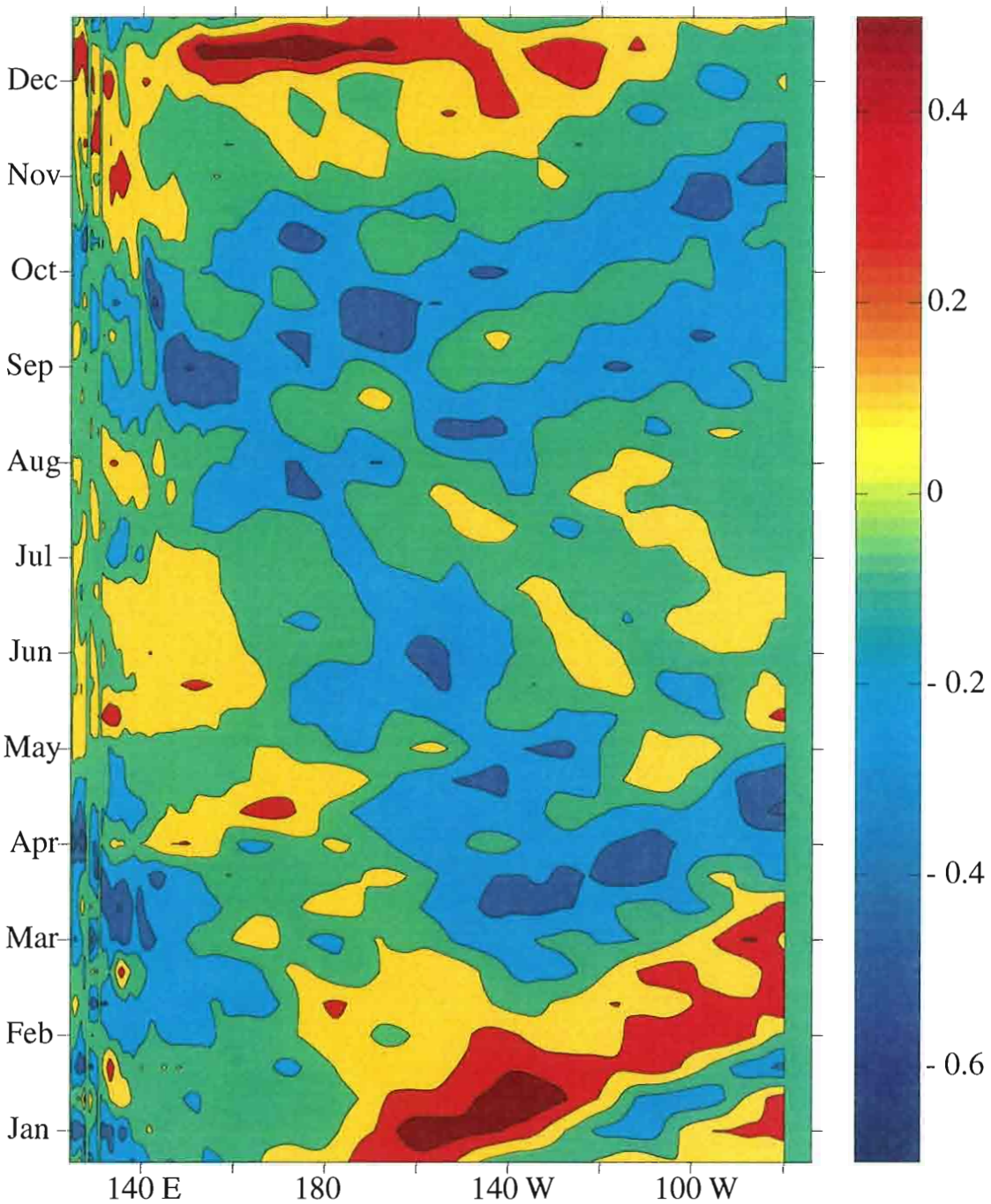

Figure 6. A Hovmuller-diagram of the annual cycle of vertical velocity along the equator across the entire Pascific basin. Note the two semiannual upwelling Kelvin waves that are generated in the west of the international dateline. One with large amplitude, generated in December, and one with less amplitude generated in April. They reach the eastern boundary in February and June respectively.

Figure 6. A Hovmuller-diagram of the annual cycle of vertical velocity along the equator across the entire Pascific basin. Note the two semiannual upwelling Kelvin waves that are generated in the west of the international dateline. One with large amplitude, generated in December, and one with less amplitude generated in April. They reach the eastern boundary in February and June respectively.

6). These waves propagate eastward and

reach the boundary 2- 3 months later,

each about a month before the two maxima in production. This means that annual remotely generated Kelvin waves, rather than the local wind forcing, controls the annual production cycle in the eastern Pacific equatorial cold tongue. Equatorial upwelling contributes to the production by keeping the thermocline shallow throughout the year.

3.1.2. Central Pacific

The region is located between 160¡ W and 120¡ W and between 7¡ N and 10 ° N. The ITCZ resides around this latitude most of the year. One expects upwelling to the north of the ITCZ and downwelling to the south of it. The overall production and the concentrations of plankton and nutrients are much lower in this region than in the Equatorial Cold Tongue (Figure 7a and c). The annual cycle in this region is not very distinct. Both production and plankton stocks are slightly higher between April and October. In this period the phytoplankton production from ammonium exceeds the production from nitrate. From Figure 7b it can be seen that zooplankton and ammonium have almost the same annual cycle, and this is also the case for phytoplankton and detritus. The vertical velocity (Figure 7c) shows a similar annual cycle to the one in the eastern Pacific with a two-three month lag. This indicates that there might be a connection between the annual cycles in the two regions. However, because the biological system responds very little to the second maximum in upwelling, the annual cycle of the biological components appear to have only one peak. The connection between the two regions is probably cause by Rossby waves reflected from the eastern boundary. The vertical velocity has a minimum between February and March, which can

between the two regions is probably cause by Rossby waves reflected from the eastern boundary. The vertical velocity has a minimum between February and March, which can

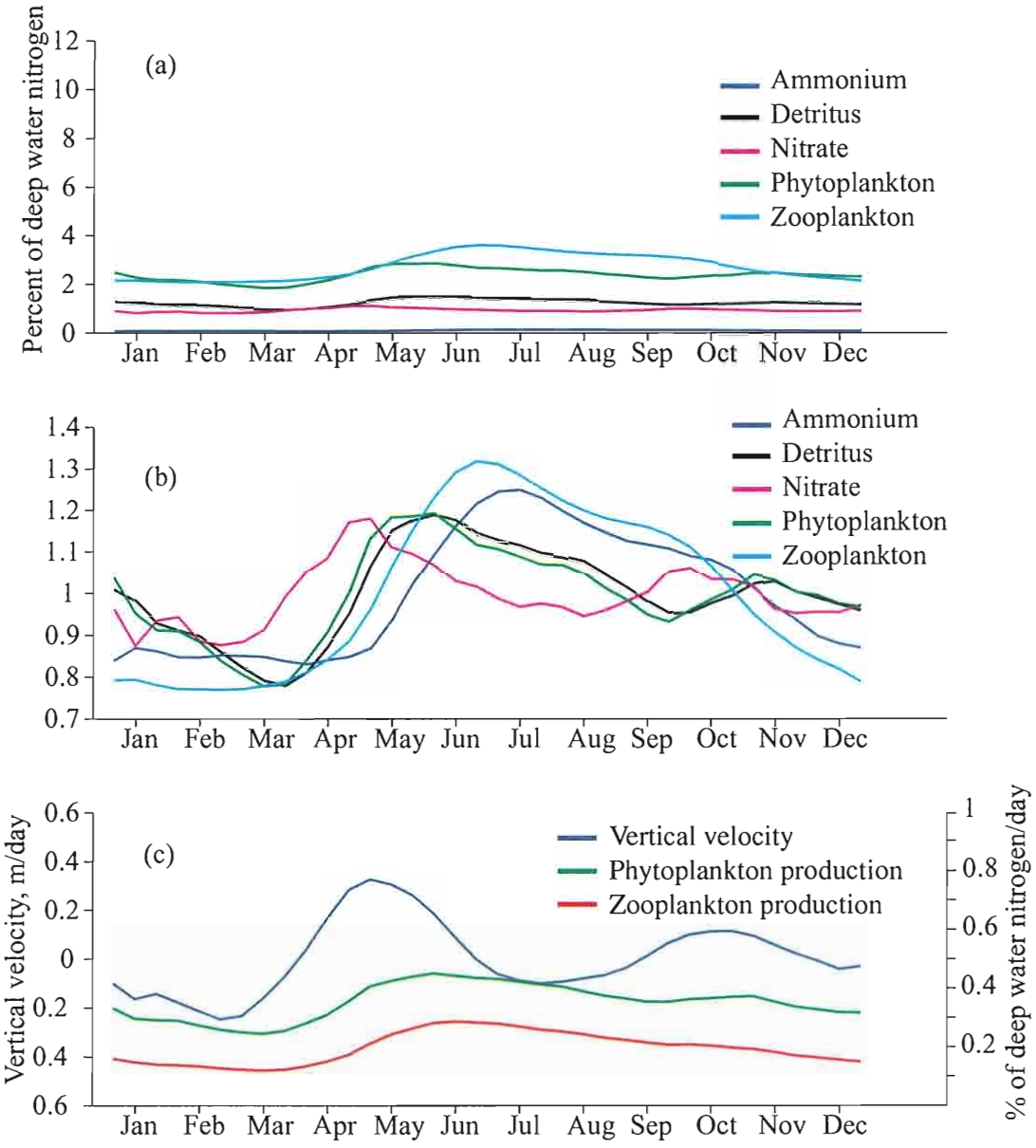

Figure 7. The annual cycle in the central Pacific of (a) each biological component, (b) each biological component scaled by its own mean value, and (c) the primary and secondary productivity and vertical velocity.

biological component scaled by its own mean value, and (c) the primary and secondary productivity and vertical velocity.

be explained by the southward movement of the ITZC. As a result of this the productivity is also lower around this period.

3.1.3. West Pacific

The third region is in the western Pacific around 6° N. The zooplankton stays very high throughout the year, keeping the stock of phytoplankton low. The production of zooplankton and phytoplankton is approximately equal (Figure 8c). As in all the regions ammonium is consistently low because phytoplankton uses ammonium faster than nitrogen.

This is the region where the North Equatorial Counter Current (NECC) leaves the western boundary. A series of eddies are generated by the shear between the NECC and the North Equatorial Current (NEC) [*Inoue and Welch*, 1993]. In addition there are two stationary eddies in this region: the Mindanao eddy and the Halmahera eddy. The large production seems to be connected to upwelling inside these eddies. Since the model has a closed western boundary the return-flow in the NECC is stronger than it should be. Therefore the shear and the strength of the eddies in the region is probably also overestimated. It remains to be seen if these eddies really can cause large biological production. Observations from 165° W around this latitude do not confirm that there is any productivity in the area [*Radenac and Rodier,* 1996]. They explain the low productivity by strong stratification caused by warm surface water, which inhibits nutrient-rich water from reaching the euphotic zone.

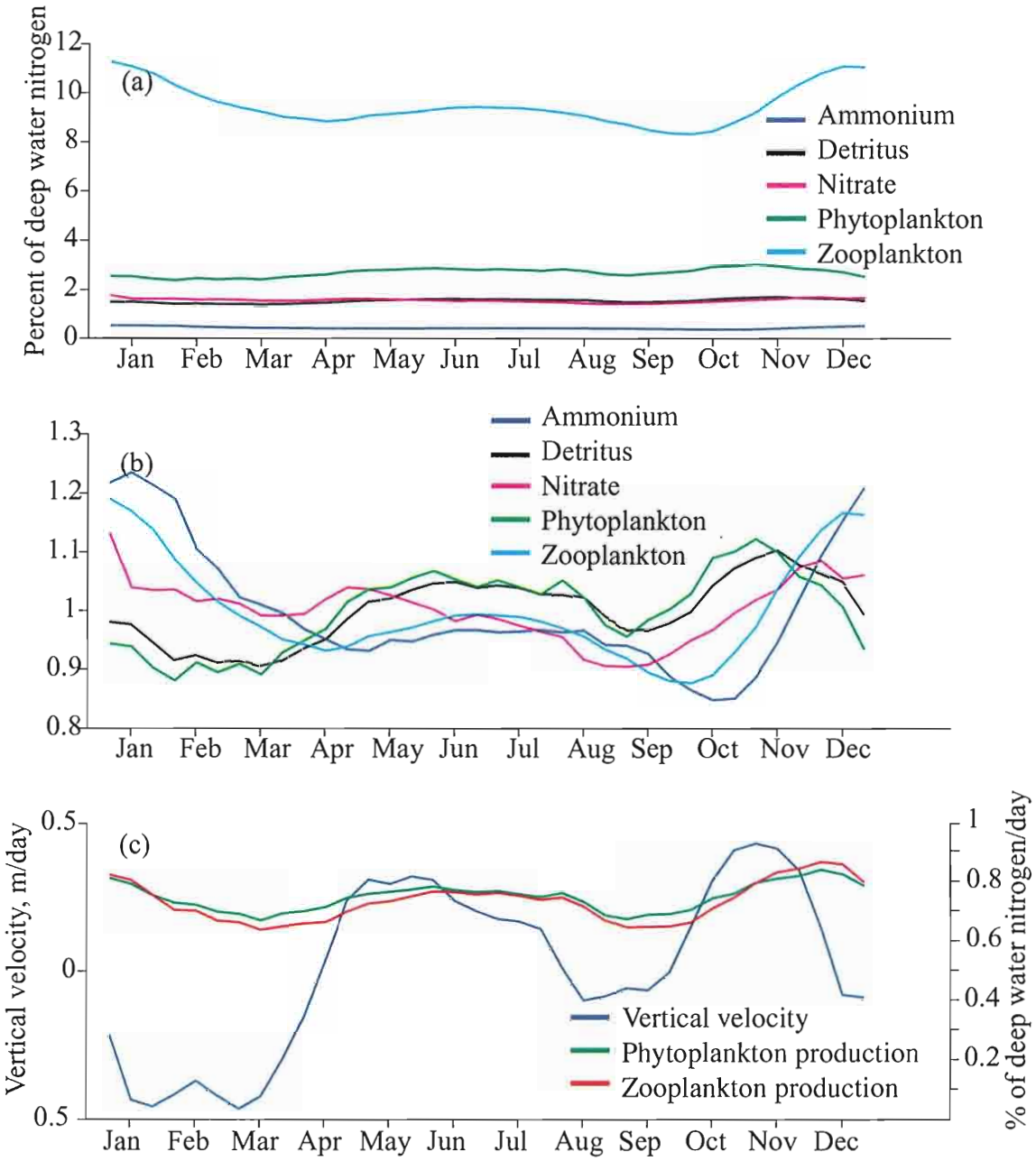

Figure 8. The annual cycle in the western Pacific of (a) each biological component, (b) each biological component scaled by its own mean value and, (c)the primary and secondary productivity and vertical velocity.

(b) each biological component scaled by its own mean value and, (c)the primary and secondary productivity and vertical velocity.

3.2. The 82-84 ENSO-event

The interannual variation connected with ENSO has a large impact on the biological production in the equatorial Pacific. Recently it has been possible to monitor this change with the help of the SeaWiFS satellite. In the 1997-98 El Niño a depletion of nutrients in the eastern Pacific during El Niño and a massive, basin-wide phytoplankton-bloom after the relaxation of the El Niño conditions were both observed in the satellite data [*Chavez et al.*, 1999]. During the 1982-83 El Niño, which peaked around Christmas 1982, a large reduction of plankton, fish, and sea birds was observed in the eastern Pacific [*Barber and Chavez,* 1983]. The reason for this is that during El Niño the thermocline is suppressed by a downwelling Kelvin waves in the eastern Pacific. This inhibits nutrient-rich water from reaching the euphotic zone. At the same time the thermocline gets shallower in the western Pacific and thus increases the biological production in the west.

The time-period of the model spans over several ENSO-events. However the 1982-83 El Niño is especially interesting, both because it has large amplitude and because the character of the biological solutions in the model changes dramatically after the end of the El Niño. Therefore this event was the main focus in the study of ENSO influences the biological system. The model shows the same decrease in biological production in the equatorial cold tongue (Figure 9) as in the SeaWiFS data [*Chavez et al.*,

production in the equatorial cold tongue (Figure 9) as in the SeaWiFS data [*Chavez et al.*,

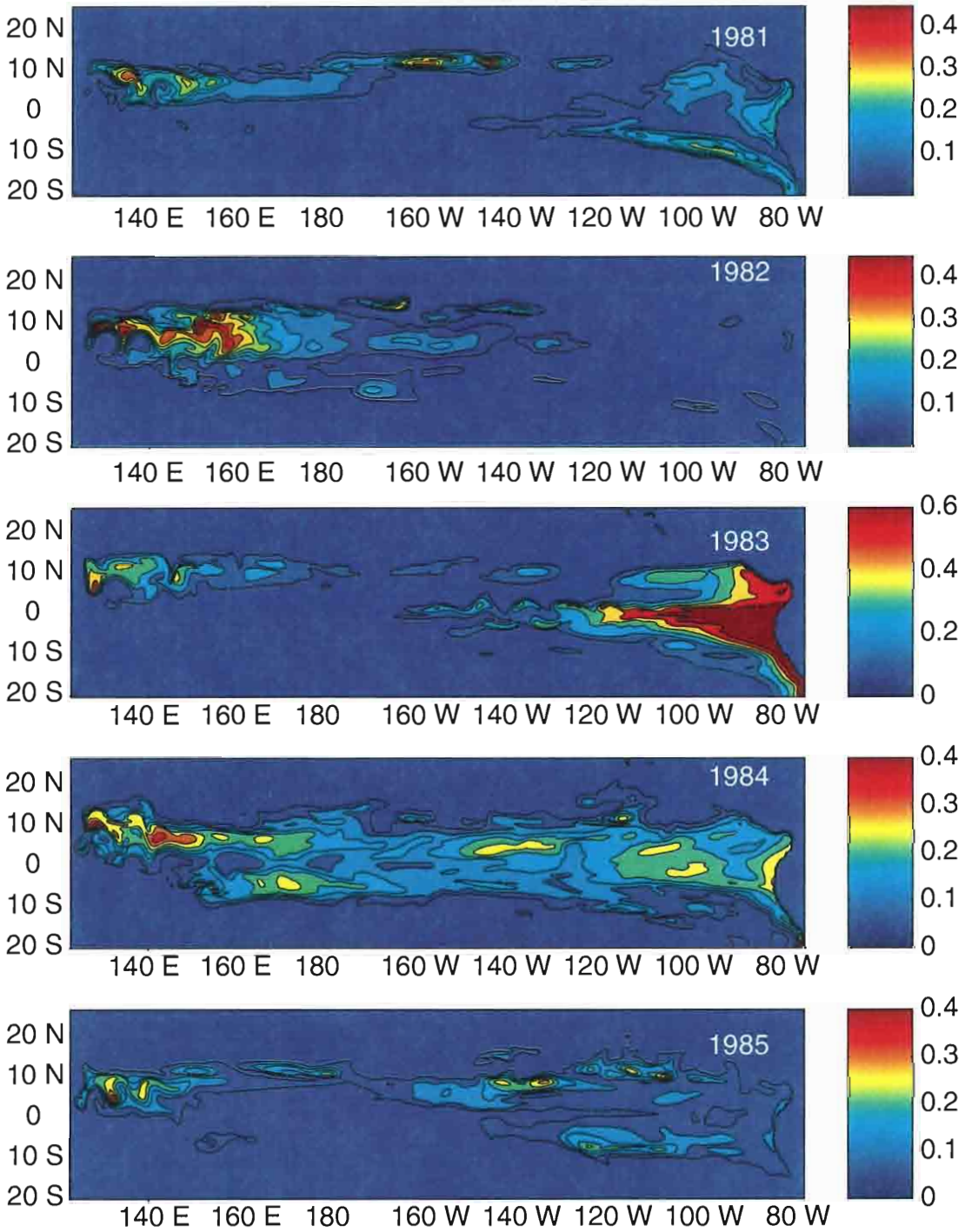

Figure 9. Snapshot of the zooplankton stock in the end of December each year from 1981 through 1985. Note that low zooplankton stock reflect low productivity and large zooplankton stock reflect large productivity

from 1981 through 1985. Note that low zooplankton stock reflect low productivity and large zooplankton stock reflect large productivity

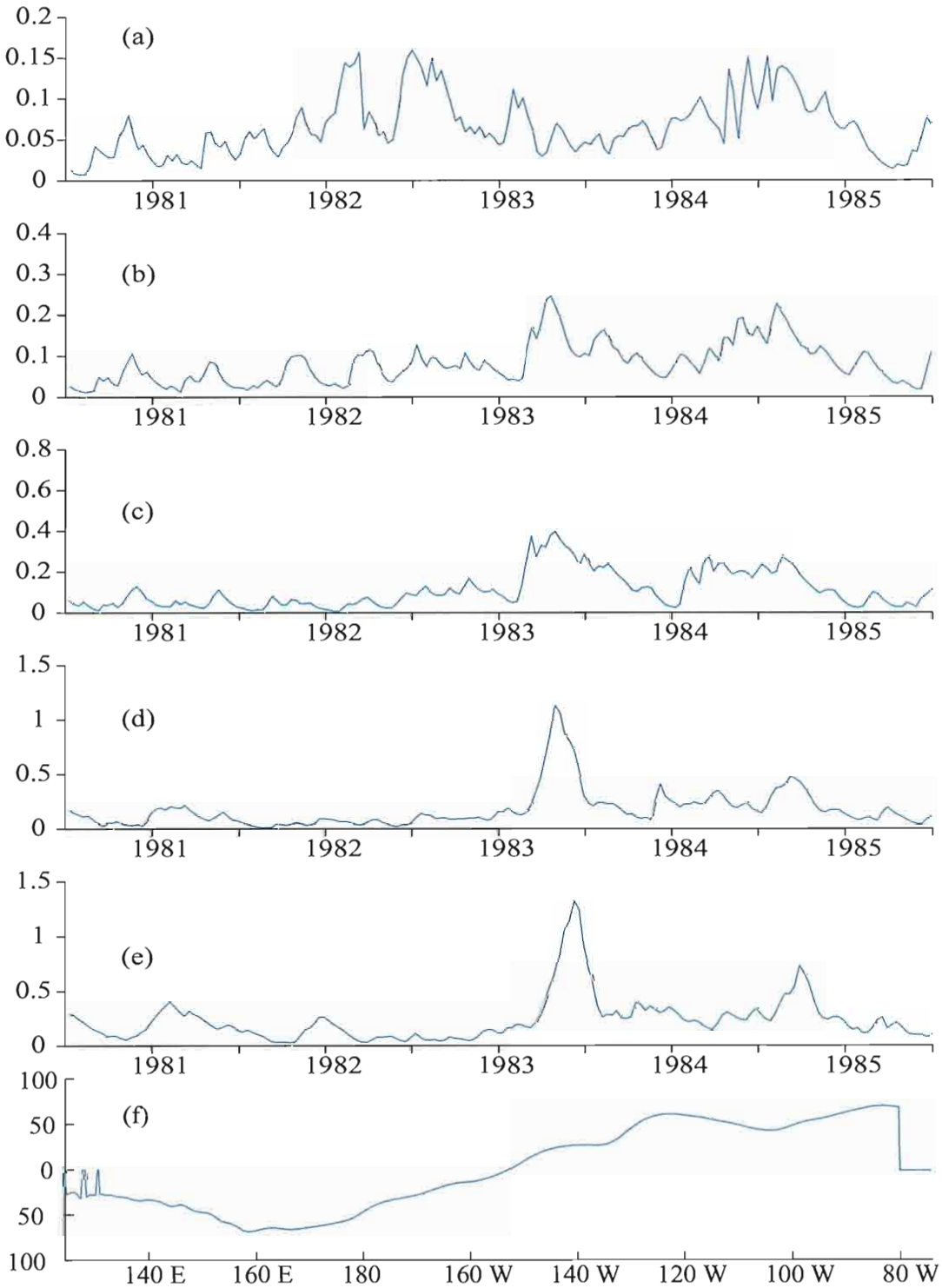

Figure 10. Total amount of nitrogen bounded up in all the biological components in the surface mixed layer (fraction of deep water nitrate-concentration) from 1981 trough 1985 along the equator at (a)150E (b) 175E, (c) 160W, (d) 135W, and (e) 110W.

Figure 10. Total amount of nitrogen bounded up in all the biological components in the surface mixed layer (fraction of deep water nitrate-concentration) from 1981 trough 1985 along the equator at (a)150E (b) 175E, (c) 160W, (d) 135W, and (e) 110W.
(f) Anomalies in the thermocline-depths (meters) along the equator in the end of 1982.

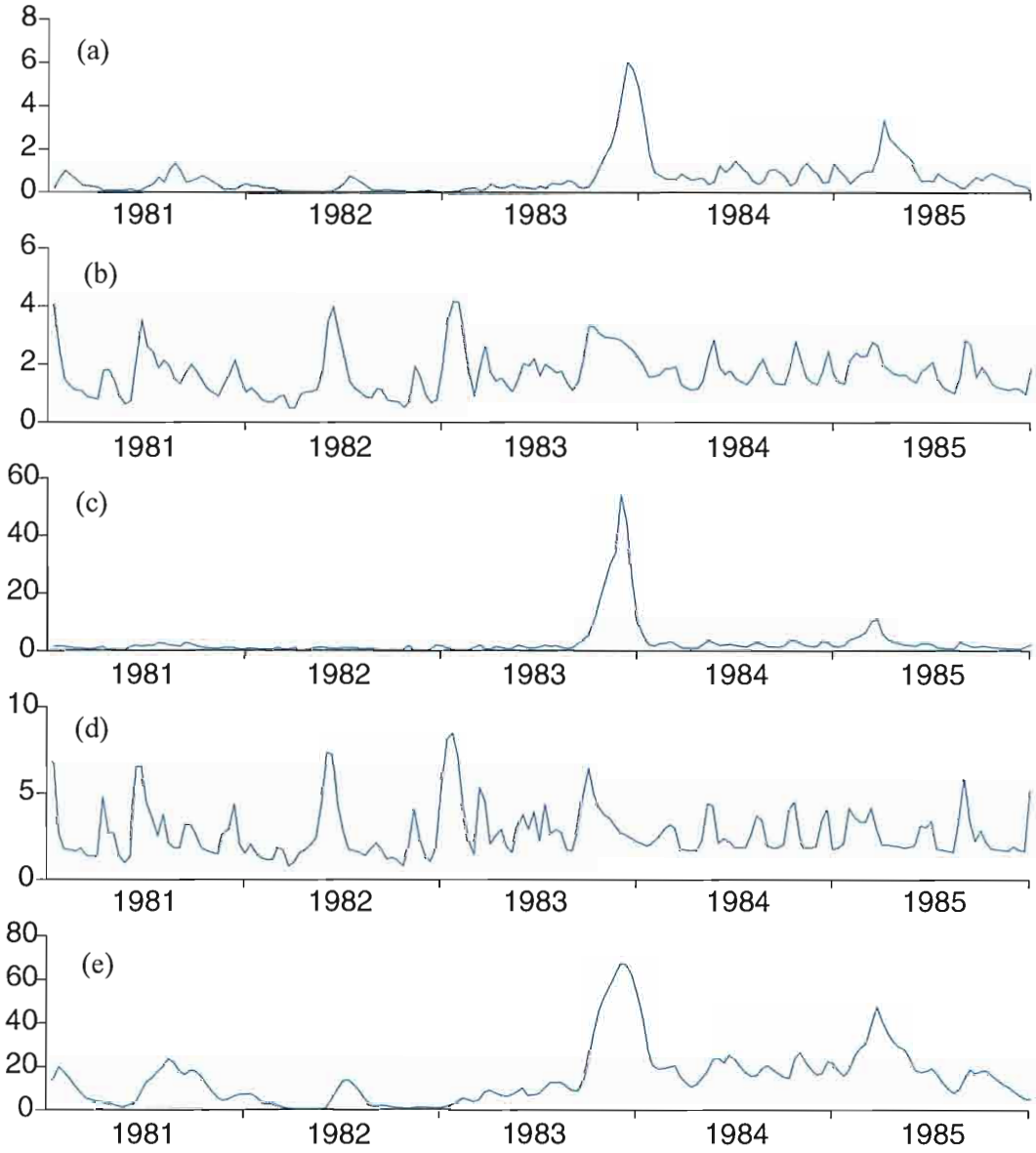

Figure 11. Time series of the biological components (% of deep-water nitrogen-concentration)from 1981 to 1986, at 110 W in the eastern Pacific on the equator of (a) ammonium, (b) detritus, (c) nitrate, (d) phytoplankton, and (e) zooplankton. Note the difference in the solutions of ammonia and zooplankton after 1983.

Note the difference in the solutions of ammonia and zooplankton after 1983.

1999]. The western region shows enhanced productivity during El Niño (Figure 10a), because the thermocline gets shallower in this region during this time (Figure 10f). In the model the reduction in the availability of nutrients is reflected in both phytoplankton stock and zooplankton stock. During the peak of the following La Niña a large amount of nitrate is added to the system by a large upwelling Kelvin wave. The Kelvin wave arrives at the coast in late 1983 and has a strong signal in both vertical velocity (Figure 14) and biological production as illustrated by zooplankton biomass (Figure 9). During this event nitrate also has a large increase because the phytoplankton stock is not large enough to use it all. The nitrate concentration is reduced to normal values very rapidly. After this event large productivity persists for more than a year along the equator. This is reflected in a persistent large stock of zooplankton. A series of reflected Rossby waves enhance the productivity north and south of the equator as they propagate westward. The model results deviate from the observed pattern in that increased upwelling after the El Niño is only reflected in the zooplankton stock (Figure 12 and 13). The event does not lead to a large phytoplankton bloom. In fact, the phytoplankton stock is smaller than normal and has lower variability during the La Niña period. The low stock is not attributed to low production, but to extensive grazing by the large zooplankton stock.

Zooplankton grows and decays on the longest time scale, so it is also the biological component that shows the most long-term variations, and also has the largest response to large upwelling of nitrate (Figure 11). In addition large amount of ammonium will be recycled from a large stock of zooplankton. Therefore the

response to large upwelling of nitrate (Figure 11). In addition large amount of ammonium will be recycled from a large stock of zooplankton. Therefore the

concentration of ammonium closely follows the population of zooplankton, especially in

periods of high productivity. Both ammonium concentration and zooplankton biomass change character after 1983. They maintain unusually large values for more a year after the large upwelling event. In contrast, phytoplankton stock and detritus remain at almost the same level. The large primary production in the period following the mature La Niña in late 1983 is caused by a series of intraseasonal Kelvin waves. (Figure 14).

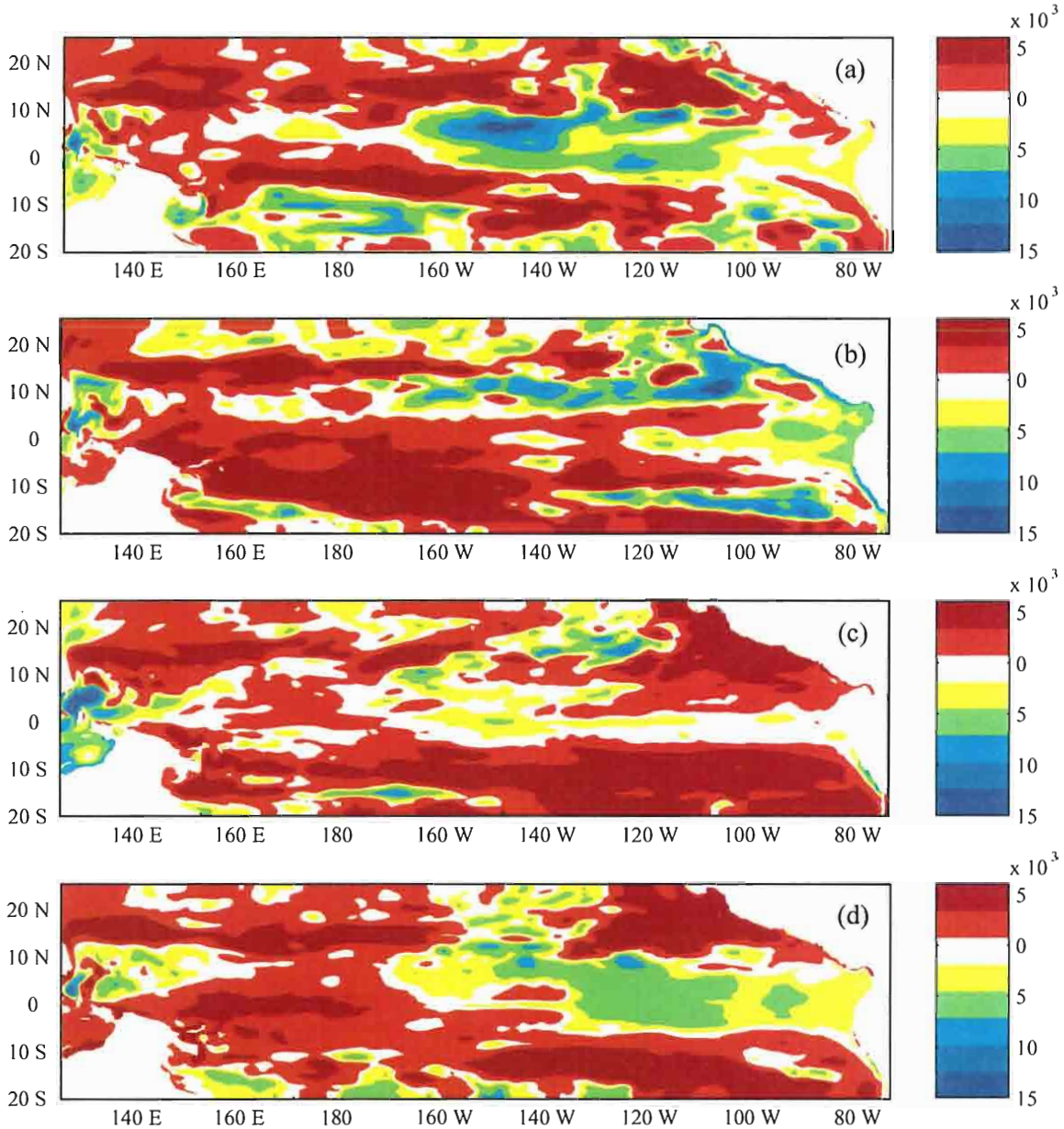

Figure 12. Annual anomalies of phytoplankton stock. The anomalies are obtained by calculating the mean over a year and subtracting the long term mean presented in section 3.1. The figures illustrates the difference in stock between an (a) a normal year (1981/1982), (b) an El Nino-year (1982/1983), (c) a La Nina year (1983/1984), and (d) a year following the La Nina (1984/1985).

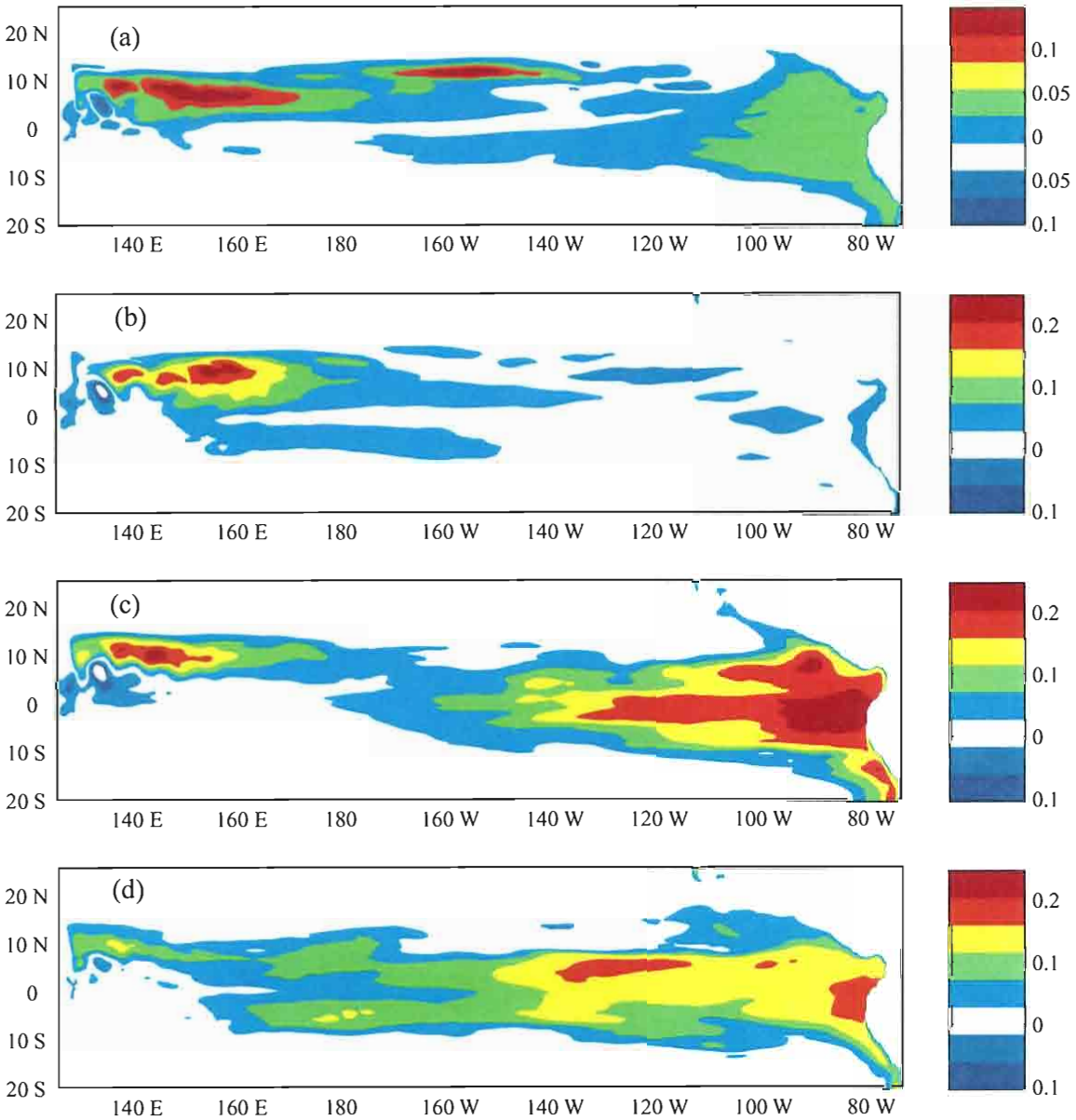

Figure 13. Annual anomalies of zooplankton stock. The anomalies are obtained by calculating the mean over a year and subtracting the long term mean presented in section 3.1. The figures illustrates the difference in stock between an (a) a normal year (1981/1982), (b) an El Nino-year (1982/1983), (c) a La Nina year (1983/1984), and (d) a year following the La Nina (1984/1985).

year following the La Nina (1984/1985).

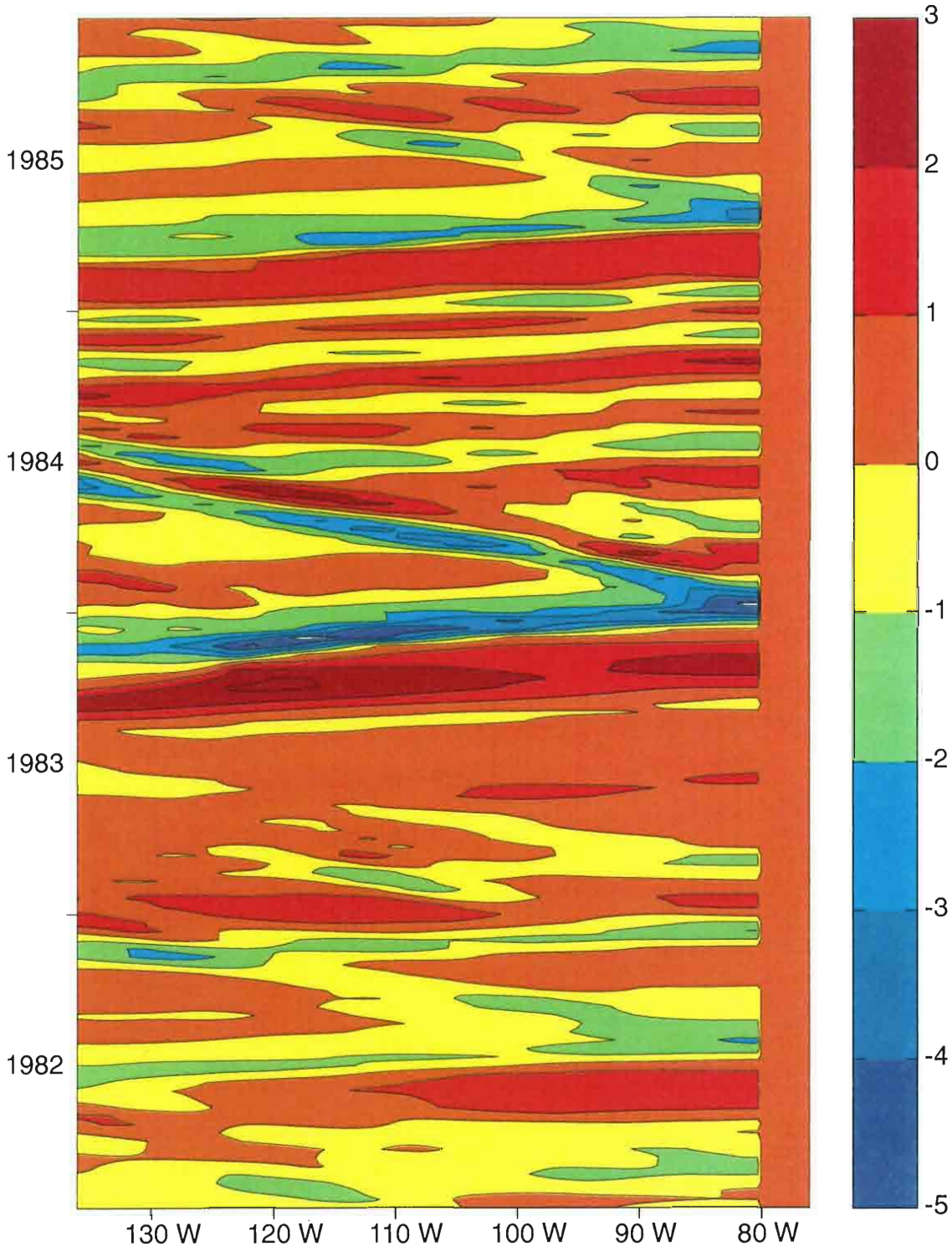

Figure 14. Hovmuller-diagram of vertical velocity at the equator, from the coast of South America to 130 degrees West in the period from 1982 through 1985. A large amplitude upwelling Kelvin wave is arriving at the coast of South America in

Figure 14. Hovmuller-diagram of vertical velocity at the equator, from the coast of South America to 130 degrees West in the period from 1982 through 1985. A large amplitude upwelling Kelvin wave is arriving at the coast of South America in
the end of 1983 and Rossby waves are reflected from it. After 1983 a series of intraseasonal Kelvin waves arrives the coast.

4. DISCUSSION

In the mean state the model results show an increase in nutrients, phytoplankton, and zooplankton from west to east. The results also show a poleward decrease of the biological components in the vicinity of equator. There is a strong asymmetry in total mixed-layer nitrogen content around the equator. This is what one would expect in comparison with observations. The mean values of phytoplankton biomass reasonably match patterns in recent SeaWiFS data [*Chavez et al,* 1999]. Both have large values in the equatorial cold tongue and north of the equator. In the model, the phytoplankton are less concentrated around the equator. In the equatorial Pacific, the satellite measurements yield values of chlorophyll *a* ranging between 0.01 and 2 mg chla/m^3 [*Chavez,* 1999]. The model results, in the mean state, are within that range. *Radenac et al.* [1996] investigated phytoplankton stock along 165° E and found that the phytoplankton stock was larger to the south of the equator in association with the south equatorial current. They also argued that the lack of productivity north of the equator was an effect of the strong stratification in that region. The stratification in the 1 1/2 layer model is the same over the whole basin. This is probably one of the reasons for the surprisingly large values that this model gives close to the NECC.

The zooplankton values are not converted to the units that can be compared with values that this model gives close to the NECC.

The zooplankton values are not converted to the units that can be compared with observations for two reasons: one is that there is uncertainty about the conversion and the

other one is that there are not much data to compare with. Figure 15 shows a composite of zooplankton observations in the Pacific Ocean. The structure is very patchy, but it does show large values around the equator and also close to the western boundary. The model probably overestimates zooplankton, especially during periods of very high nutrient-availability. The temporal variation of phytoplankton in the model can be quite large. The population can multiply by ten within a month, but after this time period the zooplankton population will have grown large enough to graze the phytoplankton stock down. In periods with large zooplankton stock, phytoplankton are unable to bloom at all. Sometimes the phytoplankton stock actually increases whenever there is low production. This is simply because there are less zooplankton around to keep the phytoplankton stock grazed down. But because phytoplankton has a fast doubling time and there are plenty of nutrients, the primary production is also high under these conditions. The concentration of phytoplankton fluctuates on much shorter time scales than zooplankton. It exhibits an annual cycle, but shows little long-term response to the ENSO events. However, the long-term response can be seen in the primary production, which in turn is reflected in the concentration of zooplankton. The lack of variation in phytoplankton biomass may be a result of the model overestimating zooplankton stock. In this model zooplankton will increase within their stock immediately after food is available. In the ocean zooplankton need more time to reproduce because they lay eggs, which take some time to hatch. A way to include this in the model would be to introduce a time-delay in the growth function for zooplankton. Another factor is that zooplankton are observed to waste more of the food when there is abundance of phytoplankton. This could be

growth function for zooplankton. Another factor is that zooplankton are observed to waste more of the food when there is abundance of phytoplankton. This could be

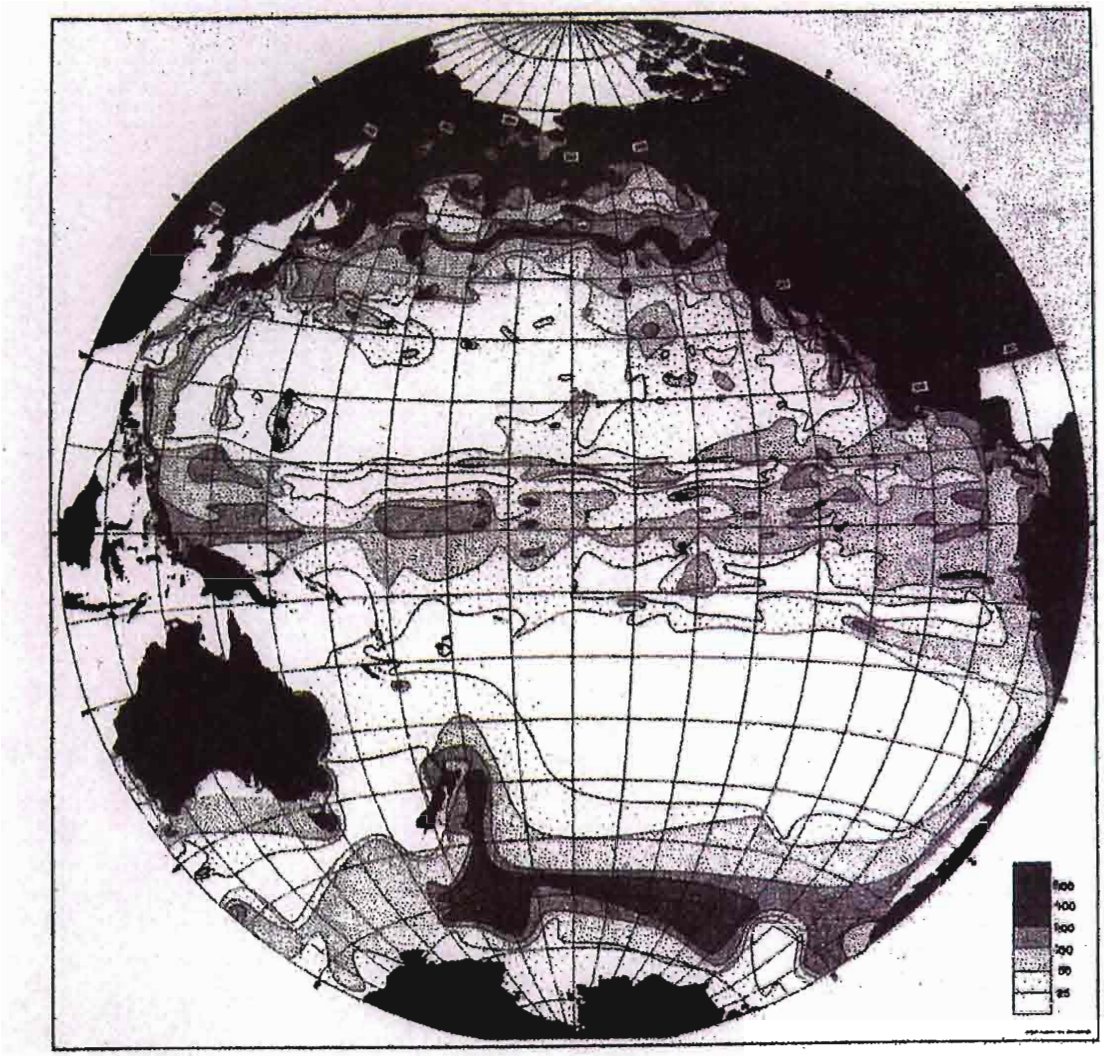

Figure 15. Distribution of zooplankton in the upper 150 meters of the Pacific Ocean (parts per 10^9 by volume). [*Reid,* 1962]

modeled by adding a food assimilation constant that is dependent on availability of phytoplankton

Disregarding light in the model has both advantages and disadvantages. On one hand it makes the model less realistic although the light-availability does not change much with season in the tropics. On the other hand one can say that the production in this model version is solely due to wind forcing. If a light cycle were added, one could distinguish the between effects of the two factors. Light affects the production in two ways, too little light will stop the photosynthesis and to much light will also inhibit the production in the part the water column nearest to the surface.

The equatorial Pacific has three regions of high productivity: the equatorial cold tongue, and two regions to the north of the equator, one in the central Pacific and one in the western Pacific. The model exhibits a distinct annual cycle in the eastern Pacific, which is connected to remotely forced waves. This response to remote forcing has been noted before on interannual time scales, in connection with El Niño, but not on an semi-annual time scale. The western and central Pacific have weaker annual cycles in. Whether or not the eddies in the west Pacific really can increase productivity is not yet clear. Similar meanders were shown by *Dadou et al.* [1996] to enhance the productivity. They coupled a physical model of the North Equatorial Current off Africa in the Atlantic Ocean with a marine ecosystem model and showed that the meandering of the current would enhance the productivity. It is possible that a similar mechanism works in the NECC in the Pacific.

Because the model has so many simplifications, the ecosystem model has its

NECC in the Pacific.

Because the model has so many simplifications, the ecosystem model has its

limitations. Some of these simplifications deal with the fact that the composition and behavior of species change between regions and as the physical environment changes. It is probably not realistic to apply the same ecosystem model to the whole basin unless more than one species are included in the model. As a general rule, large phytoplankton and zooplankton tend to dominate areas of high production while small phytoplankton and micro zooplankton tend to dominate regions with little nutrients. The tropical Pacific tends to be dominated by small (< 5 μm) phytoplankton, this is attributed to the iron limitation [*Chavez et al.*, 1996]. Zooplankton generally feed on phytoplankton, but in periods with low availability of food they can also feed on detritus. On the other hand adding too many processes would complicate the model greatly and add uncertainty. The behaviors of the species under different conditions are not well known, and can in many cases not easily be put into mathematics. The interpretation of the results also becomes more difficult. One other factor that affects the biological production is temperature. Organisms respond directly to temperature change, but an additional consideration in the tropics is that warm water is often low in nutrients.

Since there is now a satellite that provides chlorophyll data over whole ocean basins, a future study could be to run the model up to date so that the results can compared with satellite data. This will allow an evaluation of the quality of the model and will also give useful information on how to improve the model. The NSCAT-satellite provides daily wind data, so it is also possible to force the physical model with winds which will allow the model resolve higher frequency events, like the upwelling from hurricanes and tropical instability waves. This will of course also require the

winds which will allow the model resolve higher frequency events, like the upwelling from hurricanes and tropical instability waves. This will of course also require the

inclusion of the daily light cycle. Vertical structure and light-dependence may also be added to the model.

APPENDIX A

There is more than one way to represent the flux of nitrate into the mixed layer. Given the simplicity of the model, the parameterization should be kept simple. Two different parameterizations are discussed here: one is used in the model, and an alternative approach is also provided. In both cases V(N,t) is positive when the vertical velocity is upward and zero when the vertical velocity is downwards.

(a) The approach used in the model is as follows. A similarity solution is assumed between the nitrate at the bottom of the mixed layer and at the thermocline so that V(N,t) is of the following form:

$$V(N,t) = \left(\frac{dN}{dz}\left(\frac{dz}{dt}\right)'\right)\Big|_{z=-d} \tag{A.1}$$

where

$$\left(\frac{dz}{dt}\right)' = \begin{cases} 0, & \frac{dz}{dt} \le 0 \\ \frac{dz}{dt}, & \frac{dz}{dt} \ge 0 \end{cases} \tag{A.2}$$

Now assuming that nitrate decreases linearly from the base of the thermocline, where its scaled value is 1, to the base of the mixed layer, where its value is N(t), the vertical
Now assuming that nitrate decreases linearly from the base of the thermocline, where its scaled value is 1, to the base of the mixed layer, where its value is N(t), the vertical gradient of N can be estimated with:

$$\frac{dN}{dz} = \frac{N(t) - 1}{d - h(t)} \tag{A.3}$$

This formulation also makes the assumption that the vertical velocity at the bottom of the mixed layer is the same as at the bottom of the thermocline:

$$\left.\frac{dz}{dt}\right|_{z=-d} = -\frac{dh}{dt} \tag{A.4}$$

The final form becomes:

$$V(N,t) = \frac{1 - N(t)}{h(t) - d}\left(\frac{dh}{dt}\right)' \tag{A.5}$$

This parameterization has the desired property that when the upper layer is thin, or the gradient in nitrate is large, the flux of nutrients is increased. However, if the upper layer becomes very thin, V(N,t) will be very large. In addition, it is not realistic that the vertical velocities at the base of the mixed layer and at the thermocline are the same magnitude.

(b) A mass flux argument. Assume the flux of nitrate is governed by the vertical advection of nitrate, $w\frac{\partial N}{\partial z}$. Using the continuity equation to write the term in flux-form and then averaging over the mixed layer yields:

advection of nitrate, $w\frac{\partial N}{\partial z}$. Using the continuity equation to write the term in flux-form and then averaging over the mixed layer yields:

$$-\frac{1}{d}\int_{-d}^{0}\frac{\partial}{\partial z}(wN)dz = -(wN)|_{z=0} + (wN)|_{z=-d} = wN|_{z=-d} \qquad (A.6)$$

Now, under the assumption that the vertical velocity decays linearly from the bottom of the upper layer to zero at the top of the ocean, the vertical velocity will be

$$w(z) = \frac{w|_h}{h} z \qquad (A.7)$$

This gives the final form of V(N,t)

$$V(N,t) = \frac{N}{h} w(t)' \qquad (A.8)$$

where N is the deep water nitrate concentration, which has a scaled value of 1.

Comparison:

Since the nitrate concentration in the mixed layer usually is the range of 0.01 to 0.10 and the mixed layer depth is between 200 and 400 meters, the first approach usually gives a higher flux of nitrate than the second (Figure A.1). In the biological model itself the two approaches give similar solutions for detritus, nitrate, and, phytoplankton, but the second approach gives smaller concentrations for ammonia and zooplankton, in particular when the thermocline is very shallow (Figure A.2).

approach gives smaller concentrations for ammonia and zooplankton, in particular when the thermocline is very shallow (Figure A.2).

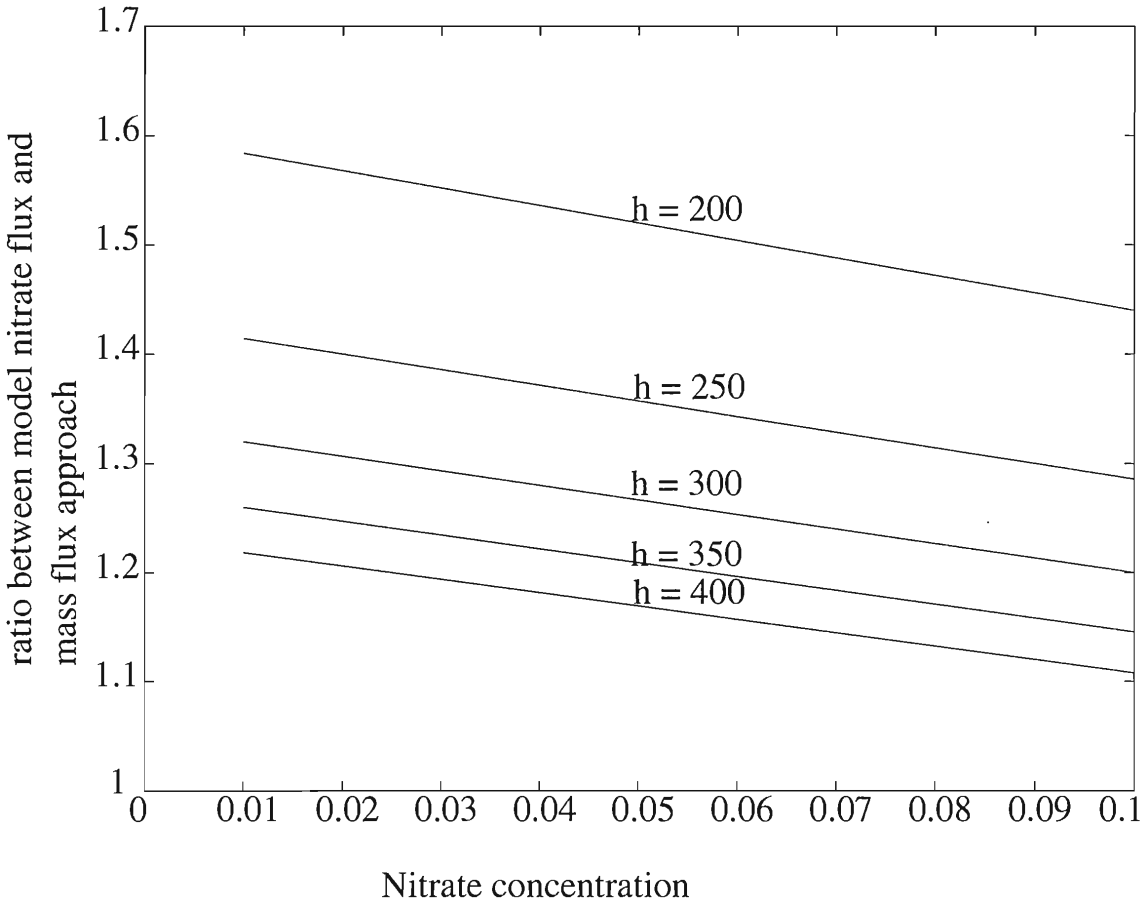

Figure A.1. The ratio between the original parameterization of vertical nitrate flux and the new parameterisation as a function of nitrate-concentration for different

Figure A.1. The ratio between the original parameterization of vertical nitrate flux and the new parameterisation as a function of nitrate-concentration for different thermocline-depths.

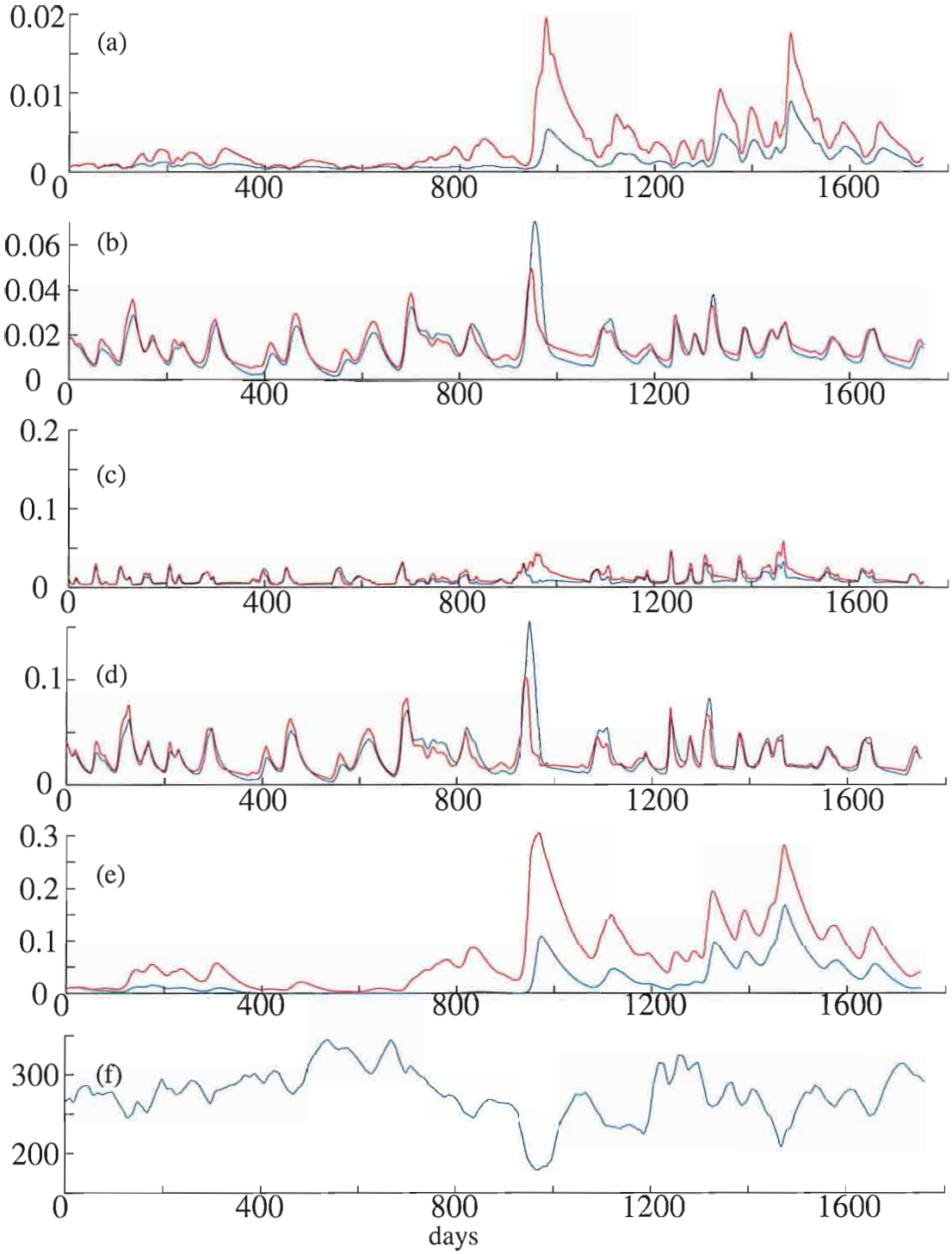

Figure A.2. The figure shows (a) ammonium, (b) detritus, (c) nitrate, (d) phytoplankton, and (e) zooplankton for the two different parameterizations of the vertical nitrate-flux. The original parameterization (red line) and the new parameterization (blue line).

Figure A.2. The figure shows (a) ammonium, (b) detritus, (c) nitrate, (d) phytoplankton, and (e) zooplankton for the two different parameterizations of the vertical nitrate-flux. The original parameterization (red line) and the new parameterization (blue line).
(f) Depth-data used in the calculation of these solutions.

APPENDIX B

The advection in the model is calculated using a semi-Lagrangian advection scheme. The concept behind this advection scheme is to integrate each biological variable along the velocity streamline intersecting with the grid point at the new timestep where the variable is calculated. The streamlines are calculated from the velocity data.

The semi-Lagrangian advection scheme approximates the total derivative in the following manner:

$$\frac{dQ}{dt} \approx \frac{Q_B^{t+1} - Q_A^t}{\Delta t} \qquad \text{(B 1)}$$

Q_B^{t+1} is the biological variable at point B, which is the grid-point that is being calculated at the new timestep. Q_A^t is the biological component at point A, which is the point where the fluid particle at was at time t. Point A is generally not at a grid point. The value of Q_A^t is calculated using bilinear interpolation. Each biological equation can be expressed in the following form:

in the following form:

$$\frac{dQ}{dt} = F(\text{Biology}, t) \tag{B.2}$$

This means that in practice the next time step in the model is calculated by following equation:

$$Q_B^{t+1} = Q_A^t + F(\text{Biology}, t)\Delta t \tag{B.3}$$

In most other biological models, false 'no-flux' boundary conditions are specified at rigid walls. Using the semi-Lagrangian advection scheme, the variables are integrated along a streamline and the streamlines will never intersect with the solid boundary, so there is no need for horizontal boundary conditions. Another advantage with the scheme is that it is unconditionally stable, in other words it is stable for all timesteps.

REFERENCES

Barber, R. T. and F. P. Chavez, Biological consequences of El Niño, *Science*, *222*, 1203-1210, 1983.

Barber, R. T, Ocean Basin Ecosystems in *Concepts of ecosystem ecology*, edited by L. R. Pomeroy and J. J. Alberts,, pp. 171-193, Springer-Verlag, New York, 1988.

Busalacchi, A. J. and J. J. O'Brien, The seasonal variability in a model of the tropical Pacific, *J. Phys. Oceanogr., 10,* 1929-1951, 1980.

Camerlengo, A. and J. J. O'Brien, Open boundary conditions in rotating fluid,*J. Comp. Phys.*, *35*, 12-35, 1996.

Chavez F.P., P.G. Strutton, G. E. Friederich, R. A. Feely, G. C. Feldman, D. G. Foley, and M.J. McPhaden, Biological and chemical responce of the equatorial Pacific Ocean to the 1997-98 El Niño, 1999.

Chavez, F.P., K. R. Buck, S. K. Service, J. Newton, and R. T. Barber, Phytoplankton variability in the central and eastern tropical Pacific, *Deep-Sea Res. 43*, 835-870, 1996.

Chai, F., S. T. Lindley, and R. T. Barber, Origin and maintenance of a high nitrate condition in the equatorial Pacific, *Deep-Sea Res., 43*, 1031-1064, 1996.

Coale, K. H., K. S. Johnson, S. E. Fitzwater, , S. P. G. Blain, T. P. Stanton, and T. L. Coley, IronEx-I, an in situ iron-enrichment experiment: Experimental design, implementation and results, *Deep-Sea Res, II, 45,* 919-945, 1998.

Cushing, D. H., The seasonal variation in oceanic production as a problem of population dynamics, *Journal du Conseil, 24*, 455-464, 1959.

Cushing, D. H, The long-term relationship between zooplankton and fish, *J. Mar. Sci., 52*, 611-626, 1995.

Cushing, D. H, The long-term relationship between zooplankton and fish, *J. Mar. Sci., 52*, 611-626, 1995.

Dadou, I, V. Gar on, V. Andersen, G. R. Flierl, and C. S. Davis, Impact of the North Equatorial Current meandering on a pelagic ecosystem: A modeling approach, *J. Mar. Res.,54*, 311-342, 1996.

Dugdale R. C. and Goering, J. J., Uptake of new and regenerated forms of nitrogen in primary productivity, *Limn. Oceanogr. 12,* 196-206, 1967.

Eppley, R. W., Standing stocks of particualar carbon and nitrogen in the equatorial Pacific at 150° W, *J. Geophys. Res., 97,* 655-661, 1992.

Fasham , M. J. R., H. W. Ducklow, and S. M. McKelvie, A nitrogen-based model of plankton dynamics in the oceanic mixed layer, *J. Mar. Res., 48,* 591-639, 1990.

Fleming, R. H., The control of diatom population by grazing, Journal du Conseil, 14, 211-227, 1939.

Friedrichs, M. A., Physical control of biological processes in the central equatorial Pacific: a data assimilative study, PhD thesis, Old Dominion University, Norfolk, Virginia, 1999.

Ivlev, V. S., Experimental ecology of the feeding of fishes, Yale University Press, New Haven. 1961.

Kamachi, M. and J. J. O'Brien, Continuous data assimilation of drifting buoy trajectory into an equatorial Pacific Ocean model, *J. Mar. Syst., 6*, 159-178, 1995.

Kindle, J. C., Equatorial Pacific Ocean variability--seasonal and El Niño time scales, The Florida State University, Tallahassee, Florida. 1979.

Koziana, V. K., A coupled bio-optical and mixed layer model for the equatorial Pacific, PhD thesis, Old Dominion University, Norfolk, Virginia, 1999.

K hn, W. and G. Radnac, A one-dimensional physical-biological model study of the pelagic nitrogen cycyling during the spring bloom in the North Sea (FLEX '76),*J. Mar. Res., 55,* 687-734, 1997.

Landry, M. R., R. T. Barber, R. R. Bidigare, F. Chai, K. H. Coale, H. G. Dam, M. R. Lewis, S. T. Lindley, J. J. McCarthy, M. R. Roman, D. K. Stoecker, P. G. Verity, and J. R. White, Iron and grazing constraints on primary production in the central equatorial Pacific: An EcPac synthesis, *Limnol. Oceanogr., 42,* 405-418, 1997.

Leonard, C. L., C. R. McClain, R. Murtugudde, E. E. Hofmann, and L. W. Harding, An [illegible] equatorial Pacific: An EcPac synthesis, *Limnol. Oceanogr., 42,* 405-418, 1997.

Leonard, C. L., C. R. McClain, R. Murtugudde, E. E. Hofmann, and L. W. Harding, An iron-based ecosystem model of the central equatorial Pacific, *J. Geophys. Res., 104*(C1), 1325-1341, 1999.

Loukos, H.,B. Frost, D.E. Harrison, J.W ; Murray, An ecosystem model with iron limitation of primary production in the equatorial Pacific at 140° W, *Deep-Sea Res.II, 44*, 2221-2249, 1997.

Martin J. H. and Fitzwater S. E., Iron-deficiency limits phytoplankton growth in the northeast pacific subarctic, *Nature 331*, 341-343, 1988.

Matear, R. J. and A. C. Hirst, Climate change feedback on the future oceanic CO_2 uptake, *Tellus Ser. B-Chem. Phys. Meteorol.*,722-733, 1999

McClain, C. R., R. Murtugudde, and S. Signorini, A simulation of biological processes in the equatorial Pacific Warm Pool at 165° E, *J. Geophys. Res., 104*(C8), 18305-18322, 1999.

Meyers, G, Annual variation in the slope of the 14-degrees-C isotherm along the equator in the pacific ocean, *J. Phys. Oceanogr., 9*, 885-891, 1979.

Radenac, M. and M. Rodier, Nitrate and chlorophyll distributions in relation to hermohaline and current structures in the western tropical Pacific, *Deep-Sea Res., 43*, 725-752 1996.

Olson, D. B abd R. R. Hood, Modeling pelagic biogeography, *Prog. Oceanogr. 34,* 131-205, 1994

Sarmiento, J. L., R. D. Slater, M. J. R. Fasham, H. W. Ducklow, J. R. Toggweiler, and G.T Evans, A seasonal three-dimensional ecosystem model of nitrogen cycling in the North Atlantic euphotic zone, *Global. Biogeochem. Cycles, 7,* 379-415, 1993.

Spitz, Y. H., J. R. Moisan, M. R. Abbott, and J. G. Richman, Data assimilation and a pelagic ecosystem model: parameterization using time series observations, *J. Mar. Syst., 16*, 51-68, 1998.

Toggweiler J. R. and S. Carson What are upwelling systems contributing to the ocean's carbon and nutrient budgets?, Environ. Sci. Res. Rep., 18, 337-360, 1995

Verschell, M. A., Mechanisms of Interannual CO_2 Flux Variability in the Equatorial Pacific Ocean, PhD, The Florida State University, Tallahassee, Forida. 1996.

Verschell, M. A., J. C. Kindle, and J. J. O Brien. 1995. Effect of Indo-Pacific throughflow on the upper tropical Pacific and Indian oceans. J. Geophys. Res.,

Pacific Ocean, PhD, The Florida State University, Tallahassee, Forida. 1996.

Verschell, M. A., J. C. Kindle, and J. J. O Brien. 1995. Effect of Indo-Pacific throughflow on the upper tropical Pacific and Indian oceans. J. Geophys. Res., *100*, 18409-18420.

Waliser, D. E. and C. Gautier, A satelite-derived climatology of the ITCZ, *J. of climate, 6,* 2162-2174, 1993.

BIOGRAPHICAL SKETCH

Annette Samuelsen was born on October 22. 1975 in Sandefjord, Norway. In the fall 1997 she completed her Cand. Mag. degree in meteorology at Geophysical Institute, University of Bergen. She began graduate school at Florida State University in the Department of Oceanography in the fall 1998.